Analysis of endoplasmic reticulum stress in rat cell models

András Balogh

Tutor: Marianna Pap

Doctoral School for Interdisciplinary Medical Sciences

Doctoral School leader: Balázs Sümegi

Program leader: József Szeberényi

2014

1 Index of contents

2 List of abbreviations

ATF4: activating transcription factor 4
ATF6: activating transcription factor 6
Bak: Bcl2-antagonist/killer
Bax: Bcl2-associated X protein
Bcl-2: B-cell lymphoma 2
Bcl-w: Bcl-2-like protein 2
Bcl-X_L: B-cell lymphoma-extra large
BFA: brefeldin A
Bim: Bcl2-interacting mediator of cell death
Bim_{EL}: Bim-extra-long
Bim_L: Bim-long,
Bim_S : Bim-short
BiP/GRP78/Hspa5: Binding immunoglobulin Protein/Glucose-Regulated Protein 78/Heat shock protein 5
Bok: BCL2-related ovarian killer
BSA: bovine serum albumin
cAMP: cyclic adenosine monophosphate
CBP: CREB-binding protein
CHOP/GADD153: transcription factor C/EBP homologous protein/ growth arrest and DNA damage-inducible gene 153
CRE: cAMP responsive element
CREB: CRE binding protein
CRTC2: CREB Regulated Transcription Coactivator 2
DTT: dithiothretiol
EGFP: enhanced green fluorescent protein
eIF2B: eukaryotic translation initiation factor 2 B
eIF2α: eukaryotic translation initiation factor 2α
ER: endoplasmic reticulum
ERAD: ER-associated protein degradation
FC: fold-change
FRET: fluorescence resonance energy transfer
G6Pase: glucose-6-phosphatase
GSK-3β: glycogen synthase kinase-3β
HS PBS: high-salt phosphate-buffered saline
HSF-1: heat shock factor-1
IC_{50}: inhibitory concentration leading to 50% inhibition
IFN: interferon
IRE1: inositol requiring enzyme 1

ISGs: IFN stimulated genes
JNK: c-Jun N-terminal kinase
Mcl-1: myeloid cell leukemia 1
MTH-68/H: more than hope-68/Hertfordshire
NDV: Newcastle disease virus
NFATc: nuclear factor of activated T-cells c
p38 MAPK: p38 mitogen-activated protein kinase
p70S6K: p70 ribosomal S6 kinase
p90RSK: p90 ribosomal S6 kinase
PBS: phosphate-buffered saline
PDK1: 3-phosphoinositide-dependent protein kinase 1
PEPCK: phosphoenolpyruvate carboxykinase
PERK: protein kinase R (PKR)-like ER kinase
PH: Pleckstrin homology
PI 3-K: phosphatidylinositol 3-kinase
PKA: protein kinase A
PKB: protein kinase B
PKC: protein kinase C
PKR: double-stranded RNA-dependent protein kinase
PUMA: p53 upregulated modulator of apoptosis
RVSM: rat vascular smooth muscle
SACO: serial analysis of chromatin occupancy
SERCA: sarco-endoplasmatic Ca^{2+}/ATP-ases
SRP: signal recognition particle
ssssDNA: single-stranded salmon sperm DNA
tATF6: truncated activating transcription factor 6
TG: thapsigargin
TM: tunicamycin
TRAF2: tumor necrosis factor receptor-associated factor 2
UPR: unfolded protein response
wt: wild-type
XBP1: X-box binding protein 1

3 Introduction

Prolonged Endoplasmic reticulum (ER) stress is a bimodal stressor. Unfavorable ER stress might lead to extensive cell loss and participates in the development of different pathological conditions, contributing to atherosclerosis, in neurodegenerative disorders, diabetes, ischaemia/reperfusion injury; on the other hand ER stress-evoked cell death is a prosperous and promising target of cancer therapy.

3.1 Protein synthesis and folding in the ER

3.1.1 Cotranslational transport in the ER

The ER takes part in the synthesis, folding and posttranslational modifications of secretory and membrane proteins in eukaryotic cells. Proteins undergo in the lumen of the ER processing and posttranslational modifications including N-linked glycosylation, lipidation, and disulfide bond formation. If a polypeptide chain is targeted to be present in the ER, its genetic code explicitly determines the cotranslational transport of the newly synthesized polypeptide chain.

These polypeptides possess an N-terminal signal sequence and are anchored during their translation to the cytosolic surface of the ER by the mediation of the signal recognition particle (SRP). The SRP is a highly conserved and ubiquitously present ribonucleoprotein complex in eukaryotic cells. The SRP is responsible for the recognition of the signal sequence motifs of the polypeptide, and targets the polysome complex to the membrane of the ER.

The SRP-polysome complex is bound by the SRP-receptor being present in the membrane of the ER. The growing polypeptide chain gets into the lumen of the ER through the Sec61 translocation channel complex. As this cotranslational transport is finished and the whole polypeptide chain translocated into the lumen of the ER, the signal peptide is cut off from the nascent protein molecule by the signal peptidase.

3.1.2 Folding in the ER

Folding of the newly synthesized polypeptide chain happens in both co- and posttranslational manner.

Sela, White and Anfinsen established more than a half century ago the science of folding with their milestone experiment declaring that folding of the bovine ribonuclease protein occurs spontaneously as the proper environmental conditions are provided. They stated that folding tends to achieve the thermodynamically most stable state of the polypeptide chain [1]. They provided evidence, that in the case of this 124 amino-acid containing bovine ribonuclease, the nucleotide sequence of the mRNA and the consequent primary structure of the polypeptide chain encodes and determines the three-dimensional structure of the mature protein.

Since then, however extensive research has been investigating this process, the whole mechanism of protein folding has not been cleared yet. Folding has been proven to be maintained and controlled by a strictly regulated and complex system in the ER, composed of numerous chaperons, foldases, isomerases, oxidoreductases, and their cofactors (reviewed in details by [2-4]).

Misfolded/unfolded proteins are restricted to enter the anterograde transport. These improperly folded proteins (containing either immature glycans, improper disulfide bonds or exposed hydrophobic domains) are identified by chaperons and aimed for degradation if the misfolded conformation persists.

Misfolded polypeptides might oligomerize, aggregate, and can be removed by autophagy. Single, not aggregating unfolded proteins are removed from the lumen of the ER and leave the ER through the translocon complex, followed by their polyubiquitination and consequential degradation termed as proteasome-dependent ER-associated protein degradation (ERAD) [5-8].

Properly folded proteins are recognized by cargo receptors and follow the anterograde transport heading the Golgi apparatus where they undergo sorting to be secretory, lysosomal or membrane proteins.

3.2 Unfolded protein response

If protein folding is disturbed, unfolded or misfolded protein molecules are retained in the ER. Physiological or pathological processes can disturb protein folding and cause retention of improperly folded proteins in the ER lumen referred to as ER stress, and a process, responding to ER stress, termed as Unfolded Protein Response (UPR) [9, 10] is activated. UPR promotes cellular adaptation by enhancing protein-folding capacity, reducing the load of the secretory pathways, and promoting degradation of misfolded proteins. However, when ER stress is extensive and/or prolonged, UPR can facilitate the activation of programmed cell death.

3.2.1 ER stress sensors of the UPR

During ER stress response there are three ER membrane-associated sensor proteins involved in the activation of signaling pathways; the activating transcription factor 6 (ATF6), the inositol requiring enzyme 1 (IRE1) and the protein kinase R (PKR)-like ER kinase (PERK). These proteins are kept in an inactive state through the direct association of their luminal domain with the ER heat shock Binding immunoglobulin Protein/Glucose-Regulated Protein 78/Heat shock protein 5 (BiP/GRP78/Hspa5) chaperon. As unfolded or misfolded proteins accumulate in the lumen of the ER, BiP molecules become sequestrated from these three sensors resulting in the activation of the UPR-related signaling pathways [9, 10] (Figure 1).

3.2.2 The IRE1 pathway

The activated IRE1 forms homo-oligomeric complexes, which leads to its autophosphorylation and activation of its RNase activity. IRE1 splices a transcription factor coding mRNA, the X-box binding protein 1 (XBP1) mRNA, which leads to the induction of UPR-related genes [9, 10]. Sustained ER stress results in the interaction of IRE1 with adaptor proteins, such as tumor necrosis factor receptor-associated factor 2 (TRAF2), which leads to the activation of the c-Jun N-terminal kinase (JNK) and p38 mitogen-activated protein kinase (MAPK) cascades, activating the apoptosis pathways (Figure 1).

3.2.3 The PERK pathway

PERK is a serine/threonine (Ser/Thr) kinase, which phosphorylates the eukaryotic translation initiation factor 2α (eIF2α) leading to the attenuation of global protein synthesis relieving the ER from the overload of proteins [11]. Phosphorylation of eIF2α selectively increases the translation of the activating transcription factor 4 (ATF4) mRNA, which regulates UPR-related genes involved in redox homeostasis, autophagy and apoptosis [12-14], among others the transcription factor C/EBP homologous protein (CHOP), also known as growth arrest and DNA damage-inducible gene 153 (GADD153) [12-14]. CHOP is a shared target gene of all three pathways of the UPR, as it can be induced by tATF6, XBP1 and ATF4. CHOP regulates the expression of several Bcl-2 family members, for example decreases the anti-apoptotic activity of Bcl-2, but increases the expression of the proapoptotic Bim [15] contributing to cell death.

3.2.4 The ATF6 pathway

Following its dissociation from BiP, ATF6 translocates to the Golgi-apparatus and is cleaved by specific proteases. The truncated, active N-terminal fragment of ATF6 (tATF6) translocates to the nucleus and upregulates the transcription of ER chaperons (e.g. BiP) and ERAD-related genes [9, 10] (Figure 1).

3.2.5 Role of Bcl-2 family members in the ER stress

ER stress mediated apoptosis is regulated by the pro- and anti-apoptotic Bcl-2 family members. The pro-apoptotic Bax (Bcl2-associated X protein) and Bak (Bcl2-antagonist/killer) proteins have a critical role in the initiation of UPR-caused apoptosis [16-18], they form a complex with the cytosolic domain of IRE1α, which is supposed to stabilize its active form [19]. Beside that BH3-only Bcl-2 family members (e.g. Bim [Bcl2-interacting mediator of cell death] and PUMA [p53 upregulated modulator of apoptosis]) cause the oligomerization of Bax and Bak leading to the permeabilization of the outer mitochondrial membrane leading to the release of cytochrome *c* and initiate the formation of the apoptosome [20, 21].

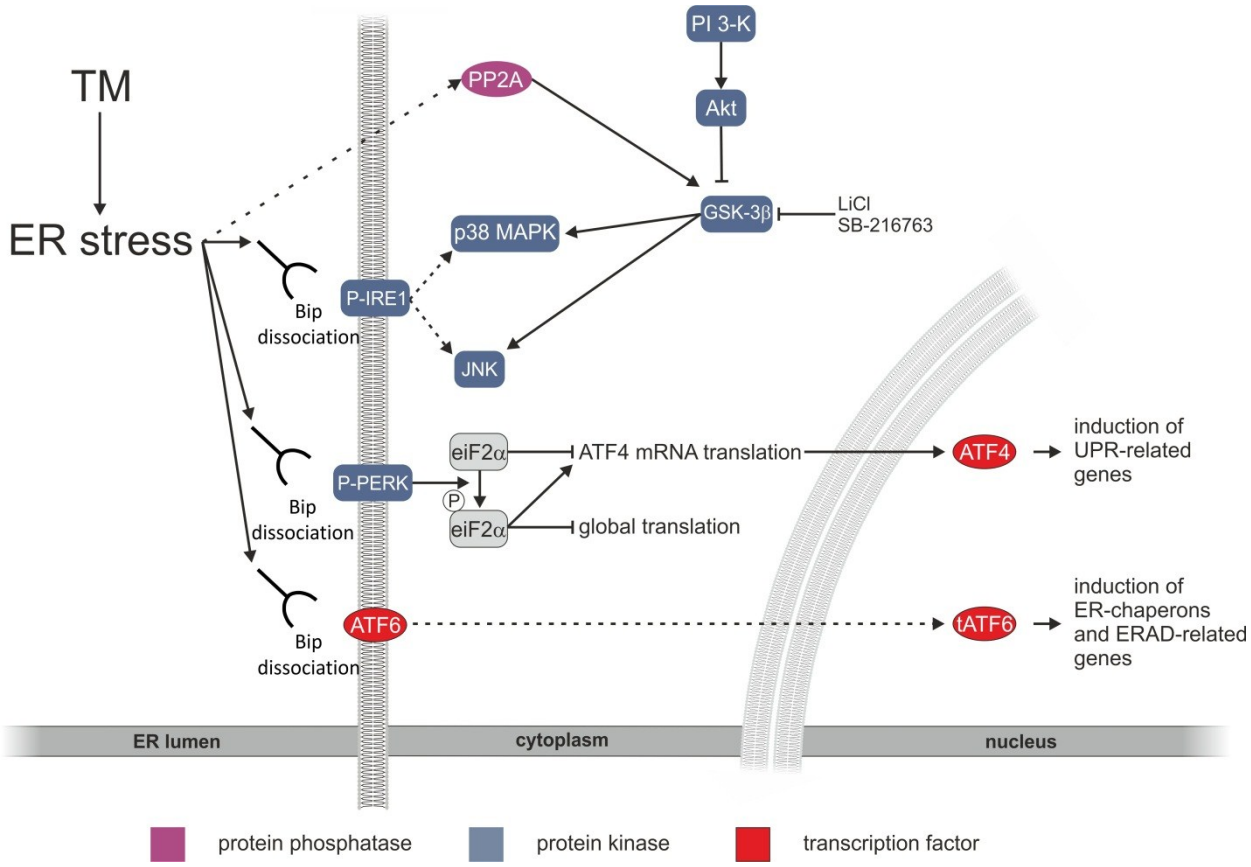

Figure 1 The signal transduction of the ER stress

3.3 The PI 3-K/Akt/GSK-3β axis and cellular survival

The phosphatidylinositol 3-kinase (PI 3-K)/Akt signaling pathway is a key regulator of numerous physiological and pathological processes including metabolism, development, proliferation, apoptosis and cell survival.

Stimulating cells with growth factors and with some cytokines leads to the increased activity of the lipid kinase PI 3-K, subsequently increasing the cell membrane's phosphatidylinositol (3,4)-bisphosphate and phosphatidylinositol (3,4,5)-trisphosphate content. These membrane-anchored lipids cause the recruitment of proteins possessing Pleckstrin homology (PH) domain, such as Akt and 3-phosphoinositide-dependent protein kinase 1 (PDK1). Akt (referred to as protein kinase B [PKB] as well, reviewed by [22]) has three isoforms (Akt1/PKBα, Akt2/PKBβ, Akt3/PKBγ) coded by distinct genes. Akt1 is widely expressed in different tissues and is mainly responsible for proliferation and

survival [23, 24]. Akt2 participates in insulin-dependent glucose homeostasis in muscle cells and in adipocytes [25, 26]. Akt3 is expressed in the testes and in the brain [27]. All three isoforms are activated upon phospholipid binding and phosphorylation on Thr308 in the activation loop and on Ser473 residues in its kinase domain by PDK1 and PDK2, respectively. Akt phosphorylates various substrates regulating a diverse set of different cellular processes including metabolism, survival and proliferation. Cell survival is thought to be regulated by Akt by phosphorylation of substrates that directly or indirectly control apoptosis pathways.

Glycogen synthase kinase-3β (GSK-3β) is a constitutively active Ser/Thr kinase that regulates important cellular processes, including glycogen metabolism, transcription, translation, cell cycle, cytoskeletal integrity and apoptosis. Activation of several signaling pathways leads to the inhibition of GSK-3β by increasing serine-9 phosphorylation (e.g. protein kinase A [PKA], Akt, protein kinase C [PKC], p90 ribosomal S6 kinase [p90RSK], p70 ribosomal S6 kinase [p70S6K]) [28]. Several substrates have been identified to be phosphorylated by GSK-3β without prior priming phosphorylation, although most of them must be prephosphorylated, "primed" four residues C-terminal to the GSK-3β phosphorylation site. Nearly 50 substrates of GSK-3β have been identified [29], including metabolic enzymes, translation initiation factor eIF2B [30], regulators of cell cycle (cyclin D1) and apoptosis (Mcl-1) and several transcription factors. Among those, c-Jun [31], nuclear factor of activated T-cells c (NFATc) [32, 33], heat shock factor-1 (HSF-1) [34] and the cAMP responsive element (CRE) binding protein (CREB) [35, 36] exhibit reduced DNA-binding affinity following phosphorylation by GSK-3β [37]. GSK-3β has been identified as a key mediator in several apoptotic signaling pathways (reviewed by Beurel E. and Jope R.S. [38]) induced by growth factor withdrawal and PI 3-K inhibition [30, 39], DNA damage [40], hypoxia [41] and ER stress [42].

3.3.1 The role of the CREB transcription factor in mammalian cells

CREB is a ubiquitously expressed leucin-zipper transcription factor that plays a critical role in the nervous system by regulating cell differentiation, proliferation, and seems to participate in the development of cancer and atherosclerosis as well [43, 44]. CREB is able to bind to the CRE sequences of DNA as a homo- or heterodimer. The kinase inducible domain contains several residues, which are responsible for the regulation of the CREB protein [45]. The most examined residue is serine-133 (S133) which is the end-point of many kinases (PKA, Akt, PKC, Ca^{2+}/calmodulin dependent kinase II and IV, MAPK, p70 S6K). Phosphorylation of S133 allows CREB to bind to the CREB-binding protein (CBP) and to the p300 enhancing gene expression. Phosphorylation of CREB at S133 creates a consensus site for phosphorylation by GSK-3β at serine-129 (S129) [46, 47]. The functional consequence of this phosphorylation is controversial. Fiol at al. [46] showed that phosphorylation of CREB at both sites is required for the full activation of CREB. In contrast, several others [35, 36, 47] found that GSK-3β negatively regulates the DNA binding activity of CREB. Activation of the PI 3-K/Akt signaling pathway leads to the inhibition of GSK-3β in PC12 rat pheochromocytoma cells [39], GSK-3β phosphorylates CREB that is thought to decrease its DNA binding activity.

3.4 ER stressors

Perturbation of ER homeostasis subsequently leads to ER stress and UPR. This might be evoked *in vivo* as well as *in vitro* by a fair set of stressors including chemical compounds, viruses, ethanol exposure, hypoglycaemia. ER stress has been proved to play a dominant role in the etiology and pathology of diverse diseases including metabolic disorders, such as diabetes, hyperlipidaemia and hypoglycaemia[48-50], degenerative disorders, including myocardial ischemia, cardiac hypertrophy, neurodegenerative diseases, cancer, inflammation and atherosclerosis [10, 51, 52].

3.4.1 Perturbation of the Ca^{2+} homeostasis

The ER is the biggest intracellular Ca^{2+} storage compartment. Affecting the homeostasis of Ca^{2+} levels in the ER leads to depletion of sarco-endoplasmatic Ca^{2+} pool leading to ER stress and UPR (reviewed recently by [53]). Depletion of Ca^{2+} can be achieved by using different chemical compounds; by the chelating agent EGTA, by the ionophores A23187

[54] and ionomycin or by thapsigargin (TG) inhibiting the function of P-type sarco-endoplasmatic Ca^{2+}/ATP-ases (SERCA) [54, 55].

3.4.2 Inhibition of protein folding

Inhibition of posttranslational modification of proteins implicitly triggers ER stress as well. Dithiothretiol (DTT) and tunicamycin (TM) are potent chemical compounds used frequently to evoke *in vitro* ER stress and UPR. DTT is a potent reducing agent interfering with disulfide-bond formation in the lumen of the ER; meanwhile TM blocks the N-linked glycosylation. TM is a mixture of N-acetyl glycosamine, uracil and fatty acid containing antibiotics [56] perturbing the function of both pro- and eukaryotic N-acetylglucosamine transferases. Homologues found in the mixture differ in the length of the fatty acid component and have different inhibitory potential. TM hinders the primary step of N-linked glycosylation by interfering with the formation of N-acetylglucosamine-dolichol (reviewed in details by [57]), leading to subsequent ER stress and UPR.

3.4.3 Ethanol exposure

Chronic ethanol exposure evokes ER stress in various organs *in vivo* including brain, liver, lung, pancreas and heart. In the organ damage ER stress plays a prominent role through the formation of acetaldehyde, oxidative stress, perturbation of Ca^{2+} homeostasis and homocystein formation [58-60].

3.4.4 Virus-evoked ER stress

Enveloped viruses use a vast array of resources of host cells and force them to produce the genomic, lipid and protein components of new virus particles. Virus infection of cells evokes a strong innate immune response and triggers ER stress as well (reviewed by [61, 62]). Viral double-stranded RNA molecules as intermediates of virus replication are recognized by the double-stranded RNA-dependent protein kinase (PKR) [63, 64] in host cells. PKR upon activation undergoes autophosphorylation, caspase-dependent cleavage and phosphorylates its target molecules including eIF2α, attenuating global protein synthesis and by means of this inhibits the synthesis of virus proteins. PKR is highly expressed in wild-type (wt) PC12 cells and its activation is triggered by a set of pro-apoptotic stimuli [65]. The

activation of PKR by viruses and the global attenuation of translation seem to be partially responsible for the antiviral effect of the cells.

PERK is a homologue of PKR and plays a crucial role in virus replication. Overloading the ER leads to the activation of PERK phosphorylating eIF2α and attenuating global protein synthesis and shutting off virus replication. The significance of PERK and eIF2α phosphorylation in the innate antiviral response is supported by the findings, discussed in references [66-68], showing that blocking eIF2α function either by the small inhibitor molecule salubrinal or by the herpes simplex virus type I viral protein ICP34.5 promotes the replication of HSV type I virus particles.

On the other hand various virus strains induce ER stress and modulate UPR in order to boost virus replication as reported previously [61, 69]. Flaviviruses, hantaviruses and paramyxoviruses, such as simian virus 5 and respiratory syncicial virus, have been reported to induce BiP expression after infection [70-75]. This phenomenon seems controversial, but only for the first glance. For the virus, it is beneficial to enhance the capacity of the ER of the cells without inducing apoptosis. Considering this, it is easily acceptable that viruses adopted and developed different strategies to modulate UPR pathways to enhance the ER capacity of the host cell in order to produce more effectively new virus particles [61] .

3.5 Oncolytic viruses

Oncolytic viruses are tumor selective viruses and are promising tools in the therapy of cancer. Meanwhile tumor cells die by apoptosis or necrosis after being infected with an oncolytic virus; normal cells are not affected. Possible mechanisms of anti-tumor activity are the following (reviewed by references [76-82]):

- Transgene expression by the viral vector,
- Viral replication-induced direct cell lysis,
- Viral protein-induced direct cytotoxicity,
- Antitumoral immune induction,
- Sensitization to chemotherapy and irradiation.

Oncolytic viruses have been reported to be safe and effective according to clinical (phase I-III) trials conducted so far. The first virus which was introduced into the clinical therapy

was the genetically engineered ONYX-015 adenovirus strain, selectively killing p53 negative tumor cells, with promising results. Different viruses have been postulated to possess potential anti-tumor activity, as listed below, containing genetically engineered, normally occurring and attenuated virus strains.

- Adenoviruses (e.g.: ONYX-015, H101, CGTG-102, Ad5-Delta24GD, CV706, CV787),
- Reoviruses (e.g.: Reolysin)
- Herpes simplex virus (e.g.: Talimogene, Iaherparepvec, NV1020, H103) ,
- Poxviruses (eg.: Vaccinia JX-594 , Vaccinia GL-ONC1, Vaccinia GM-CSF),
- Picornaviruses (e.g.: Seneca Valley virus),
- Newcastle disease virus (strains: MTH-68/H, PV701, NDV-HUJ),
- Vesicular stomatitis virus.

Newcastle disease virus (NDV) belongs to the family of Paramyxoviridae. The virus is enveloped and it is surrounded by a phospholipid bilayer acquired from the cell membrane of the host cell during the process of particle budding. NDV is reported to enter cells both by direct membrane fusion and caveola-mediated endocytosis [84]. Virus particles contain a negative single-stranded 15.1 kb sized RNA genome; they are pleomorphic, sized from 50 to 500 nm in diameter [83].

In humans NDV does not cause diseases (except for mild flu-like conditions), while in natural avian host species NDV causes severe pandemias among wild and domesticated bird populations. The attenuated NDV vaccine strain MTH-68/H (more than hope-68/Hertfordshire) [84] has a selective cytotoxic effect on transformed mammalian cells resulting in apoptosis [85, 86]. *In vitro* studies in our laboratory previously indicated that tumor cell lines showed a wide range of sensitivity toward MTH-68/H infection [85]. MTH-68/H vaccine treatment prolonged survival of patients with advanced cancer resistant to conventional therapeutic protocols [87], thus MTH-68/H might be a promising future tool for cancer therapy considering its following features:

1. MTH-68/H is non-pathogenic in humans.
2. MTH-68/H does not show signs of antigene recombination.
3. The genome of NDV viruses does not integrate into host cells genome excluding the possibility of random integration and insertional mutagenesis.
4. MTH-68/H has been reported to induce apoptosis in a p53-independent manner [85].

Individual case studies, phase I and II clinical trials were conducted using PV701, MTH-68/H and NDV-HUJ strains with varying therapeutic response [84, 87-95]. MTH-68/H showed promising results in glioblastomas [84, 87, 94] and has been thought to have immune modulation properties, direct lytic and pro-apoptotic effect, although the proper mechanism of action has not been perfectly understood so far. It is still a question why some of the tumors responded well; meanwhile other tumors remained resistant toward NDV therapy.

4 Aims

The experiments and findings of the current thesis aimed to characterize ER stress in rat cell cultures. For the experiments two different approaches were used.

I. TM blocks N-linked glycosylation in the ER leading to subsequent ER stress and UPR. GSK-3β has been postulated as a key molecule in the signal transduction of ER stress as well as a modulator of the activity of CREB through the phosphorylation of CREB on residue S129. Considering the possible relation between the GSK-3β-mediated ER stress and the significance of the S129 and S133 CREB phosphorylation sites, the following points were aimed to be investigated in rat cell culture models.

a) Stable transfection of PC12 cells with expression vectors coding for wtCREB and mutant CREB proteins.
b) Determination of the IC_{50} and IC_{80} concentrations of TM were determined in wtPC12 cells using ATP assay.
c) Comparison of the survival rate of wtPC12 cells, wtCREB overexpessing and mutant CREB expressing PC12 lines were compared using ATP assay and apoptosis assay after TM treatment.
d) Analysis of the activation of different ER stress/UPR related signaling pathways.
e) Study the role of GSK-3β in the signal transduction of ER stress was examined in wtPC12 cells, in wtCREB overexpressing and mutant CREB expressing cell lines using GSK-3β inhibitors LiCl or SB-216763 or applying GSK-3β specific knock-down technique.
f) Examination the different cell lines the expression of different Bcl-2 family member proteins was studied after TM treatment.
g) Observe the association of the Bcl-2 family member Bim protein to the microtubule network was studied with confocal microscopy.

h) Determination of the survival rate of primary rat vascular smooth muscle cells, Rat-1 fibroblasts and wtPC12 cells transiently transfected with wtCREB coding expression vector and treated with TM with or without LiCl.

II. It has been known that the attenuated Newcastle disease virus MTH-68/H strain induces ER stress in PC12 cells [85]. The following points were aimed to be studied after infecting wtPC12 cells with MTH-68/H particles.

a) Characterizing the gene expression alterations of wtPC12 cells with transcriptome analysis using cDNA chip after 12 hours of MTH-68/h infection.
b) Verifying the result of the chip using qRT-PCR.
c) Identifying altered signaling pathways upon MTH-68/H infection using functional gene cluster analysis.

5 Materials and methods

5.1 Cell culture

PC12 rat pheochromocytoma cells (kindly provided by G.M. Cooper, Boston University, Boston, MA, USA) were cultured in Dulbecco's Modified Eagle's Medium (Sigma, St. Louis, MO, USA) containing 4500 mg/l glucose, 4 mM L-glutamine and 110 mg/l sodium pyruvate and supplemented by 5% foetal bovine serum and 10% horse serum (Gibco, Carlsbad, CA, USA), referred to as high serum containing medium throughout the thesis. Cells were used between passage 5 and 20 for the experiments.

Wild-type or mutant CREB expressing stable cell lines were cultured in the presence of 200 µg/ml G418-sulphate. 5×10^6 cells/100-mm plates (Greiner, Frickenhausen, Germany) for Western blot analysis, 10^5 cells/well on 24 well plates (Greiner, Germany) for apoptosis assay, 10^4 cells/well on 96 well plates (Greiner, Germany) for immunocytochemistry and 2×10^3 cells/well on white flat-bottom 96 well plates (Greiner, Germany) for ATP assay experiments were plated 24 hours prior to the experiments. Cells were used between passage 3 and 15 for the experiments.

Rat-1 cells were cultured in RPMI-1640 medium containing 10% newborn calf serum (Gibco) (Sigma, USA) supplemented with 90.91 U/ml penicillin, 90.91 ng/ml streptomycin and 18.18 ng/ml gentamycin (Sigma). Cells were used between passage 8 and 15 for the experiments.

Primary rat vascular smooth muscle (RVSM) cells were isolated from 7 week old Sprague Dawley male animal. After removal of the aorta, the vessel was washed in medium 199 (Sigma) containing 10% FBS (Biochrom, Berlin, Germany), followed by the mechanical removal of the adipose tissue. Aorta was digested in 1×PBS containing 2 ml 1.4 mg/ml collagenase (Sigma) and 1.4 mg/ml elastase (Serva, Heidelberg, Germany) at 37°C for 10 minutes. After the enzymatic digestion the sample was placed into medium 199 and the tunica adventitia was removed from the tunica media. The surface of tunica media was scraped carefully with a scalpel in order to remove residual fibroblasts. The remaining part was cut into small pieces and the tissue pieces were placed into 1 ml of 1×PBS containing 2 mg/ml collagenase and 1 mg/ml elastase for 20 minutes at 37°C. After incubation 10 ml medium 199 was added and cells were pelleted by centrifugation followed by a second

wash/centrifugation step using medium 199. Cells were cultured further in SmGM medium (Lonza, Basel, Switzerland) supplemented with SmGM-2, EGF, FGF, insulin, gentamycin/amphotericin B SingleQuotes-2 (Lonza). Smooth muscle phenotype of the culture was validated using smooth-muscle-actin specific immunolabeling (Figure 2).

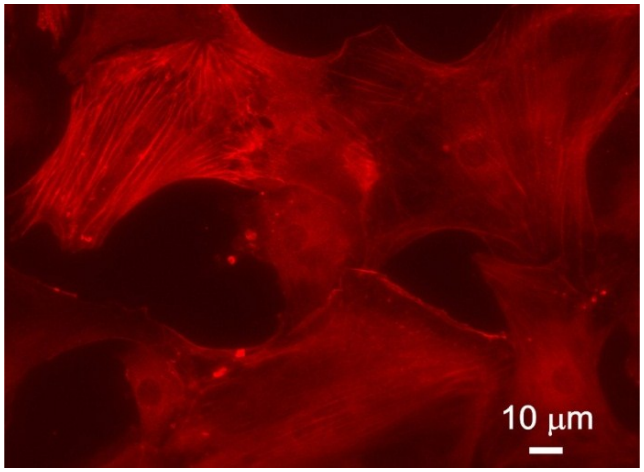

Figure 2 Validation of cell-type of primary RVSM cells
Primary RVSM cells were plated on poly-L-lysine coated coverslip containing wells. 24 hours later cells were fixed and indirect immunocytochemistry was performed using 1:100 monoclonal smooth-muscle-actin specific antibody, clone 1A4 (Dako, Hamburg, Germany) and 1:250 Cy3-conjugated anti-mouse secondary antibody (Jackson). Cells were visualized by Zeiss Axio Imager.M2 fluorescence upright microscope using 20× Plan-Apochromat objective (NA 0.8). Bar denotes 10 μm.

5.2 Infection of PC12 cells with attenuated MTH-68/H Newcastle disease virus for gene-expression analysis

For the exon-chip analysis PC12 cell cultures (10^6 cells in 60-mm plates) were infected with highly purified batches of the NDV strain MTH-68/H described in detail by Fábián et al [85]. Infections were performed at the IC_{50} value for PC12 cells (12.87 particles/cell; [96]) for 12 hours.

5.3 Site-directed mutagenesis

Site-directed mutagenesis of the pcDNA3/RSV-FlagCREB vector (a kind gift from M.E. Greenberg, Harvard Medical School, Boston, MA, USA) was conducted using Stratagene's QuickChange Site-Directed Mutagenesis kit (Agilent Technologies, Santa Clara, CA, USA), according to the manufacturer's instruction. Primers used for mutagenesis were

synthesized by Invitrogen (Carlsbad, CA, USA). The applied sequences were the followings (mutations are indicated with bold letters): S129A forward primer: 5'-GGGAAATTCTT**GCC**AGGAGGCCTTCC-3', S129A reverse primer: 5'-GGAAGGCCTCCT**GGC**AAGAATTTCCC-3', S133A forward primer 5'-GGAGGCCT**GCC**TACAGGAAAATTTTG-3', S133A reverse primer: 5'-CAAAATTTTCCTGTA**GGC**AGGCCTCC-3'. Mutagenesis was validated by sequencing.

5.4 Stable transfection of cells

5×10^6 PC12 cells were seeded onto 100-mm plates 24 hours prior to transfection. A day later cells were transfected with 9 μg of pcD/RSV-FlagCREB, pcD/RSV-FlagCREB S129A, pcD/RSV-FlagCREB S133A and pcD/RSV-FlagCREB S129A-S133A respectively, together with 11 μg carrier salmon sperm single stranded DNA (ssssDNA), using the calcium phosphate precipitation method [97]. Three days after transfection, wtCREB and mutant CREB expressing cells were cultured for 4 weeks in the presence of 400 μg/ml G418-sulphate (Gibco). Separate clones were picked and subclones were cultured and checked for expression. Clones showing the highest expression of CREB in Western blot analysis were selected for further experiments (Figure 3).

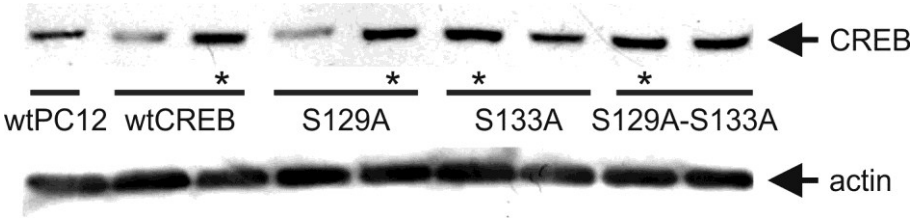

Figure 3 CREB expression in wtPC12 cells and in the various CREB constructs transfected cell lines

Expression levels of wtPC12 and CREB overexpressing cells. WtPC12 and stably transfected cell lines were lysed; proteins were isolated and subjected to Western blot analysis using an anti-CREB antibody as described in the Materials and methods. Clones labeled with an asterisk were chosen for further studies. Actin specific antibody was used as a loading control. The experiment was repeated for three times. A representative Western blot is shown.

5.5 Preparation and coating of coverslips

Coverslips were washed with 200 μl 96% ethanol for 5 minutes on a rocker. Ethanol was removed and coverslips were washed with 200 μl distilled water for five minutes on a

rocker. After discarding water 200 µl of 13 µg/ml poly-L-lysine (Sigma, St. Louis, MO) was pipetted onto the coverslips. Plates containing coverslips were placed in a 37˚C humid thermostate for 30 minutes. After removal of the poly-L-lysine solution, coverslips were washed 3 times for 5 minutes with distilled water. Plates were left overnight under UV light inside the cell culture cabinet.

5.6 Confocal microscopy

10^4 cells/well were seeded onto poly-L-lysine coated plastic coverslips in 96-well plates (Greiner) in high serum containing medium, which was exchanged to a medium containing 0.5% horse serum (low serum containing medium throughout the thesis) 24 hours later. Next day cells were treated with TM (Sigma) in 200 µl low serum containing medium according to the appropriate figure legend. After the treatment cells were fixed in 200 µl 4% paraformaldehyde in 1xPBS and left at room temperature for 15 minutes. Then the samples were kept at 4˚C overnight. Next day paraformaldehyde was removed and samples were washed with 1×PBS for 5 minutes. Non-specific antibody binding sites were blocked by adding 100 µl 10% bovine serum albumin [BSA (Sigma)] in high salt 1×PBS (1×PBS containing 23.38 g extra NaCl/l referred later as HS PBS). Samples were gently shaken at room temperature for 1 hour on a rocker. CREB and CHOP specific primary antibodies (CellSignaling Danvers, MA, USA) were added in a dilution of 1:200 dissolved in 3% BSA HS PBS, 20 µl/well. Samples were incubated overnight at 4°C. Next day samples were washed 3 times for 5 minutes in HS PBS. Secondary, fluorophore-conjugated antibodies (Jackson ImmunoResearch Laboratories, West Grove, PA, USA) were added to the samples in a final concentration of 1:200 dissolved in 3% BSA HS PBS. Samples were gently shaken overnight in the dark at 4°C on a rocker. Non-specifically bound secondary antibodies were removed by washing the samples 3 times for 5 minutes in HS PBS on a rocker. Samples were mounted onto coverslips using Vectashield (Vector Laboratories, Burlingame, CA, USA) anti-fading mounting medium and visualized by an Olympus FluoView 1000 confocal laser scanning fluorescence microscope (Olympus, Center Valley, PA, USA). Fluorophores were excited in photon counting and sequential mode creating single-plane images. For negative control, samples were incubated only with the secondary antibody (Figure 4).

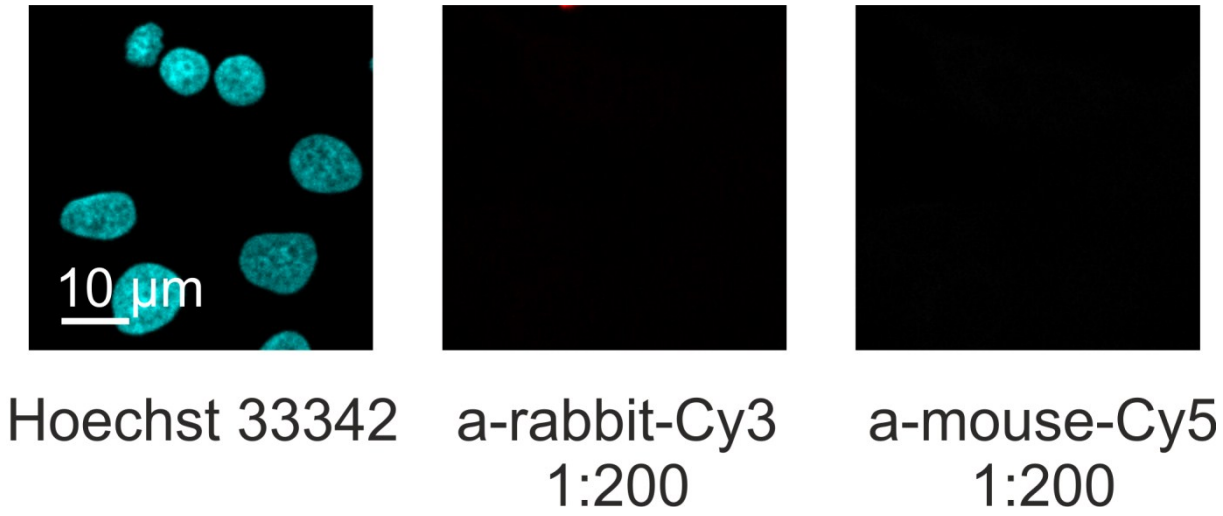

Figure 4 Confocal single-layer images showing negative controls for immunocytochemistry
Cells were cultured and plated on Thermanox coverslips as described in the Materials and methods. Samples were incubated without primary antibodies, in the presence of Cy3-conjugated anti-rabbit and Cy5-conjugated anti-mouse secondary antibodies followed by Hoechst 33342 DNA staining. Samples were visualized by Olympus FluoView 1000 confocal laser scanning fluorescence microscope. Representative images are shown. Bar denotes 10 µm.

5.7 ATP assay

Cell viability was tested by a luciferase-based ATP assay (Promega, Madison, WI). 2×10^3cells/well were seeded onto poly-L-lysine coated white-wall F-bottom 96-well plates (Greiner, Frickenhausen, Germany). Next day the medium was replaced by a low serum containing medium for 1 day. Afterwards cells were treated with TM according to the figure legend. 24 hours after the treatment 100 µl media were left in the wells. Before the measurement plates were placed to room temperature for 30 minutes. FluoStar Optima plate reader (BMG Labtech, Offenburg, Germany) measured 100 µl freshly prepared ATP assay reagent mixture into the wells. Plates were shaken for 2 minutes with 300/minute frequency. Plates were then incubated at 25°C for 10 minutes before reading and fluorescence of the wells was measured with a gain of 3000.

5.8 Apoptosis assay

10^5 cells/well were seeded onto poly-L-lysine coated glass coverslips containing 24-well plates. Next day the medium was changed and stable transfected cells were incubated in low serum containing medium, transiently transfected cells in high serum containing

medium for 24 hours. Cells were treated with TM as indicated in the figure legend. 24 hours later cells were fixed in 4% paraformaldehyde in 1×PBS. Cell nuclei were stained by Hoechst 33342 (Calbiochem, Darmstadt, Germany) fluorescent DNA dye in the final concentration of 0.5 μg/ml. The percentage of apoptotic nuclei was determined by counting at least 200 cells/sample in randomly chosen viewfields using Olympus BX61 fluorescence microscope (Olympus, Center Valley, PA, USA). For representative normal and apoptotic nuclear morphology see Figure 5.

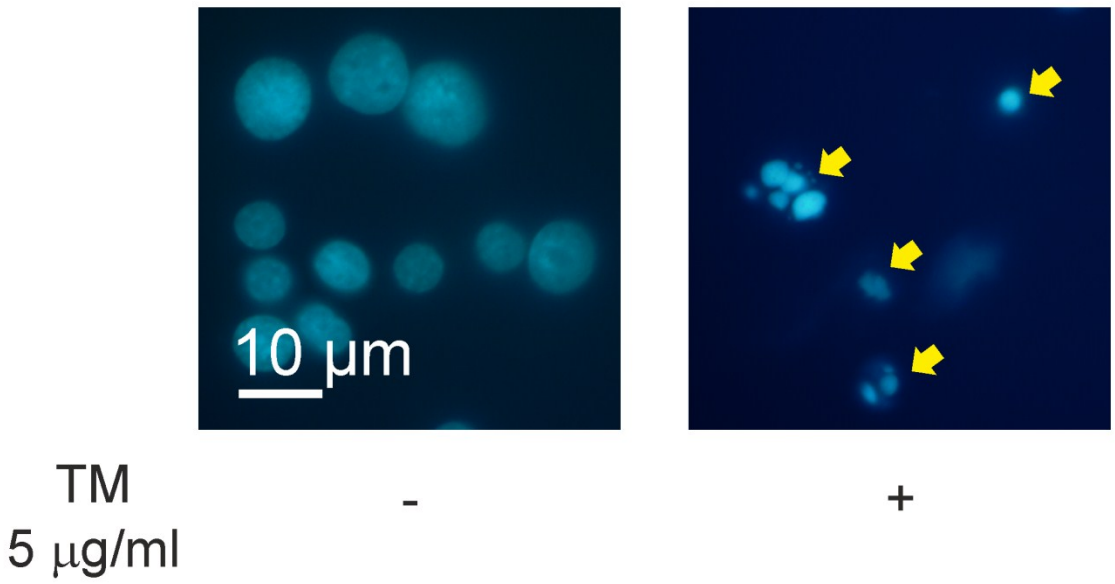

Figure 5 Normal and apoptotic nuclear morphology
WtPC12 cells were seeded onto poly-L-lysine coated glass coverslips and left untreated or were treated with TM for 24 hours as described in the Materials and methods and processed for Hoechst 33342 DNA staining. Arrows show apoptotic nuclei. Bar denotes 10 μm.

5.9 Western blot analysis

5×10^6 cells were plated, kept in low serum containing medium for 24 hours and then treated with TM for 24 hours as described in the figure legend. Cells were lysed in M-Per mammalian protein extraction buffer (Thermo Scientific, Waltham, MA, USA). 40 μg of protein lysates were loaded onto 12% SDS-polyacrylamide gels and transferred onto PVDF membranes (Amersham, Buckinghamshire, UK). The following primary antibodies were used: anti-CREB, anti-actin, anti-BiP, anti-P-JNK, anti-P-p38 MAPK, anti-P-eIF2α, anti-P-

GSK-3 Ser9, anti-P-CREB S129, anti-P-CREB S133, anti-Bim, anti-Bcl-2, anti-Bcl-w, anti-Bcl-X_L, anti-Bok purchased from CellSignaling (Danvers, MA, USA, 1:1000 final dilution), anti-Mcl-1 purchased from Sigma (final dilution 1:500) anti-ATF6 and anti-P-IRE1 purchased from AbCam (final dilution 1:500).

Species specific horseradish peroxidase-conjugated secondary antibodies (CellSignaling) were used at 1:2000 final dilution and the immunocomplexes were visualized by Pierce ECL Western Blotting Substrate (Thermo Scientific). Protein bands were quantified with Kodak 1D software (version 3.5.5.B). Results were normalized to actin levels.

5.10 Knockdown of GSK-3β using siRNA technique

5×10^5/well wtPC12 cells were plated for RT-qPCR into 6-well plates and 2.5×10^4 cells/well for apoptosis assay and immunocytochemistry onto Thermanox (Thermo Scientific) coverslips placed into 24 well plates. Next day transfection was performed using 1 μl/ml DharmaFECT 1 (Thermo Scientific) transfection reagent and 5 μl 20 μM ON-TARGETplus Non-targeting Pool and GSK-3β specific siGENOME SMARTpool siRNA (Thermo Scientific) according to the manufacturer`s instructions. The following day the medium was changed to low serum containing medium supplemented with 87 U/ml penicillin and 87 ng/ml streptomycin (Sigma). 24 hours later cells were treated with 5 μg/ml TM for one day or left untreated and samples were processed for further analysis**.** Knockdown of GSK-3β was validated by immunocytochemistry and qRT-PCR. For immunocytochemistry samples were incubated with anti-GSK-3β antibody (CellSignaling, 1:250) and Cy3-conjugated anti-rabbit antibody (Jackson). Cells were visualized by Zeiss Axio Imager.M2 fluorescence upright microscope using 40× Corr M27 dry Plan-Apochromat objective (NA 0.95). Samples were analyzed with the same exposure time and settings. GSK-3β expression was characterized by measuring mean signal intensity/cell measured by ImageJ v. 1.47 (National Institute of Health, Bethesda, MD, USA).

5.11 FRET analysis

Slides for immunocytochemistry were prepared using mouse anti-tubulin (Merck, Darmstadt, Germany) and rabbit anti-Bim (CellSignaling), Cy5-conjugated anti-mouse and Cy3-conjugated anti-rabbit antibodies (Jackson ImmunoResearch Laboratories, West Grove,

PA, USA) at 1:200 dilution as described in the Confocal microscopy section of Materials and methods. Samples were mounted onto glass slides using 50% glycerol dissolved in 1×PBS. Imaging was conducted using Olympus FluoView 1000 confocal laser scanning fluorescence microscope. Fluorophores were excited with He and Ne lasers with 90% transmissivity. Signal of pre- and post-bleaching images was collected using 40× UPlan FLN objective (NA 0.75) creating 1024×1024 pixel single-layer images in photon count mode. Excitation of each pixel was 10 μs. Range of interest was randomly selected and samples were bleached with 4× zoom with 20 μs/pixel excitation until 90% decrease in the fluorescence of the acceptor was not reached. FRET efficiency and fluorophores' distance was calculated by Olympus FV 10-ASW Ver.01.07.01.00 software (Olympus, Center Valley, PA, USA). Experiments were repeated three times.

5.12 Transient transfection of cells with expression constructs

5×10^4 wtPC12, Rat-1 or primary RVSM cells were plated onto 24-well plates containing poly-L-lysine coated coverslips in 500 μl final volume and cotransfected in suspension with pcDNA3 (LifeTechnologies, Grand Island, NY, USA) and pEGFP-C1 vectors (Clonetech, Mountain View, CA, USA) (mock-transfected) or with pcDNA3-FLAG-CREB and pEGFP-C1 constructs (CREB-transfected). 3.3-3.3 μg plasmid was mixed with 465 μl SmGM-2 medium followed by the addition of 20 μl FuGENE HD transfection reagent (Promega, Madison, WI, USA). The mixture was incubated for 10 minutes at room temperature and then cells were transfected with 37.5 μl/well transfection mixture. 24 and 48 hours after the transfection media was changed and cells were treated according to the figure legend of Figure 20. Cells were fixed and stained as described in the Apoptosis assay section of Materials and methods. The efficiency of transfection was above 80% (Figure 6).

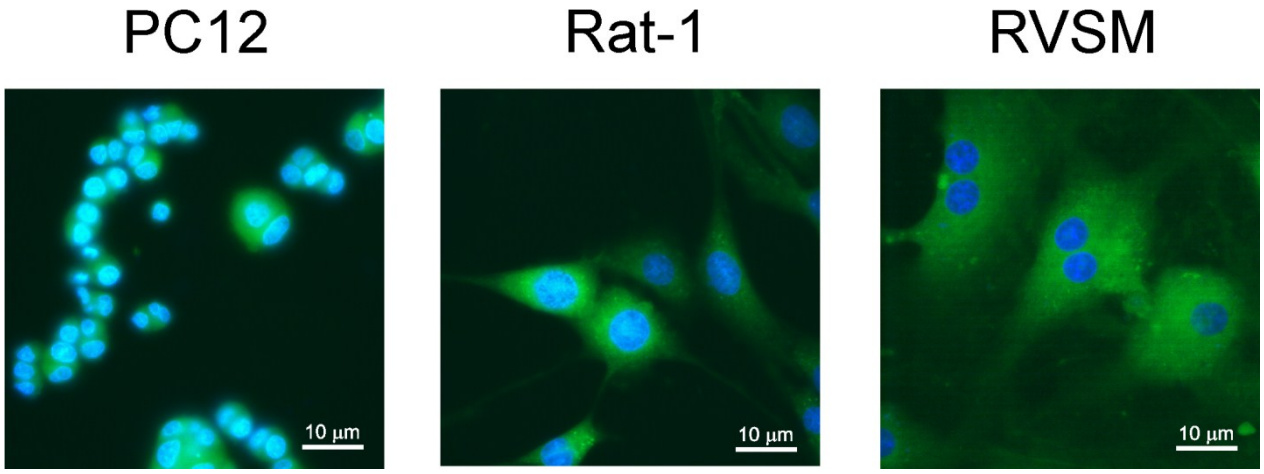

Figure 6 EGFP expression in transient transfection experiments in different rat cell lines
Cells were transfected with pcDNA3-CREB and pEGFP-C1 vectors. Samples were analyzed by Zeiss Axio Imager.M2 fluorescence upright microscope using 40× Corr M27 dry Plan-Apochromat objective (NA 0.95). At least 100-150 EGFP positive cells/sample were counted and analyzed according to nuclear morphology. Figure shows a representative result 72 hours after transfection. Blue color indicates cell nuclei stained with Hoechst 33342, green color shows EGFP expression. Bar denotes 10 μm.

5.13 Exon chip analysis

Total cytoplasmic RNA from control and MTH-68/H-infected PC12 cell culture triplicates was isolated using Qiagen's (Hilden, Germany) RNeasy kit according to the manufacturer's instructions. Samples were analyzed on Affymetrix platform using Affymetrix GeneChip Rat Exon 1.0 ST Array chip (Santa Clara, CA) by UD-Genomed Ltd (Debrecen, Hungary). Expression of specific genes was determined from raw microarray data. Gene expression data were normalized and the absolute fold-change expression (FC) was determined. At least 2-fold increase or decrease in expression was considered to be significant using unpaired T-probe with Benjamini-Hochberg correction. Functional categorization of genes with altered expression was performed by the DAVID functional annotation clustering tool [25] using the recommended settings of the tool. A total of 729 genes were found up-regulated by 12-hour MTH-68/H treatment (FC 2.00-100.0), while the number of virus-down-regulated genes was 612 (FC 2.00-3.9). Genes not recognized by the tool were excluded from analysis.

5.14 RNA extraction and quantitative reverse transcriptase PCR

Total RNA was isolated using the RNeasy RNA isolation kit (Qiagen) according to the manufacturer's instruction. Concentration of isolated RNA was measured by NanoDrop-1000 spectrophotometer (Thermo Scientific, Waltham, MA). Purity of the isolated RNA was confirmed by measuring the absorbance ratio at 260nm (A260) and 280nm (A280). RNA samples possessed A260/A280 values greater than 1.8 and were considered to be pure for further analysis. Two micrograms of total RNA were used for cDNA synthesis using High Capacity cDNA Reverse Transcription Kit (Life Technologies, Carlsbad, CA) in a 20 µl final volume according to the manufacturer's instructions. SYBR Green or TaqMan analysis was conducted in duplicate using an Applied Biosystems 7500 Sequence Detector (Life Technologies). Each 10-µl SYBR Green reaction mixture contained 4 ng of cDNA, 5 µl of Fast SYBR Green Master Mix (Life Technologies) and 300 nM primer. TaqMan assay reactions contained 4 ng of cDNA, 5 µl of TaqMan Fast Universal Master Mix (Life Technologies), 300 nM primer and 150 nM probe in 10µl final volume. For TaqMan assay amplification conditions were performed according to a protocol consisting of an initial 2 min denaturation step (95^{o}C) followed by 40 cycles of denaturation (3 s, 95^{o}C) and annealing (20 s, 60^{o}C). For SYBR green assay prior to amplification uracil-N-glycosylase was activated by a 2 min long step at 50^{o}C followed by polymerase activation at 95^{o}C for 20 s. Further on 40 cycles of denaturation (3 s, 95^{o}C) and annealing (30 s, 60^{o}C) were performed. In cases of SYBR Green protocol melting curve analysis was performed, which resulted in single products confirming the specificity of the amplification reaction. The expression levels of the target genes were normalized to 18S ribosomal RNA levels and were calculated using the standard curve method. Primers and probes were designed using Primer Express software 3.0 (Applied Biosystems, Carlsbad, CA) and were synthesized by Biotez (Berlin, Germany). Primer and probe sequences are listed in Table 1.

Gene	NCBI accession number	Forward/Reverse	Probe
Bmyc	NM_001013163.2	F: 5'-AGGAGACGCGGTGAAGCA-3' R: 5'-CCACATACAGTCCTGCAGAATGA-3'	-
Casp12	NM_130422.1	F: 5'-CAGTCCTCCGACAGCACATTC-3' R: 5'-GCTTCACCCCACAGATTCCTT-3'	-
Cdc26	NM_001013240.2	F: 5'-GCGACGAAAGCCAACTCGCC-3' R: 5'-CGGGCCTCCAGGTCCTTTCG-3'	-
Ddx58	NM_001106645.1	F: 5'-CCCAGAAATATGAGCAGTGGATT-3' R: 5'-TCATCTTTGTCAGGCATCTGAAA-3'	-
Mrpl34	NM_001006965.1	F: 5'-ATCCTGTTGAGTGGCAGGTATCTC-3' R: 5'-TTGCTCGGCTGATACTCGTTT-3'	-
Pole2	NM_001169108.1	F: 5'-GTGTTTCATGCCAATGCCTTT-3' R: 5'-ATTAATATTTCCATAGTATGCCCTTGTG-3'	-
Stat2	NM_001011905.1	F: 5'-CTACACCAAGGAAGTGCTACAGTCA-3' R: 5'-TCTTCGGCGAGAACCTGGTA-3'	-
Tnf	NM_012675	F: 5'-CCTCACACTCAGATCATCTTCTCAA-3' R: 5'-CGCTTGGTGGTTTGCTACGA-3'	5'-FAM-ACTCGAGTGACAAGCCCGTAGCCCA-TAMRA-3'
Ifnb1	NM_019127.1	F: 5'-GCGTTCCTGCTGTGCTTCTC-3' R: 5'-TGCTAGTGCTTTGTCGGAACTG-3'	5'-FAM-CACTGCCCTCTCCATCGACTACAAGCAG –TAMRA-3'
18S	NR_046237.1	F: 5'-ACATCCAAGGAAGGCAGCAG-3' R: 5'-TTTTCGTCACTACCTCCCCG-3'	5'-FAM-CGCGCAAATTACCCACTCCCGAC-TAMRA-3'
Gsk3b	NM_032080.1	F: 5'-CAGAGGCAATCGCACTGTGT-3' R: 5'-CACAAGCTTCCAGTGGTGTTAGC-3'	-

Table 1 Primer pairs and probes used to validate the expression of selected genes by quantitative reverse transcriptase PCR

5.15 Statistical analysis

Statistical analysis was conducted using GraphPad Prism 5.03 (GraphPad Software, La Jolla, CA, USA) and SPSS 13.0 (SPSS, Chicago, IL, USA). Determination of normal distribution was conducted by Kolmogorov-Smirnov test. Statistical significance was confirmed by one-way ANOVA followed by Bonferroni posthoc test if significance was observed. Data were expressed as mean ± SEM. $P<0.05$ value was considered statistically significant.

6 Results

6.1 Increased CREB nuclear occupancy

PC12 cells were transfected with wtCREB or different phosphorylation site CREB mutant expressing plasmids. Serine at the position of 129 and 133 were exchanged to alanine by site-directed mutagenesis one by one or together, which renders those mutants non-phosphorylatable forms of CREB. PC12 cells expressing the wtCREB, Ser129Ala-CREB, Ser133Ala-CREB and the double mutant Ser129Ala-Ser133Ala-CREB (referred throughout the thesis as wtCREB, S129A CREB, S133A CREB and S129A-133A CREB, respectively) constructs showed a substantially higher CREB expression compared to wtPC12 cells in Western blot experiments (Figure 3). Clones labeled with an asterisk in Figure 3 were selected for further studies expressing a comparable amount of the CREB protein. In comparison to the wtPC12 cells the CREB expression levels of the different CREB construct-transfected cell lines showed 1.7-1.8 fold increase determined by densitometry of the Western blots showing the CREB expression level of the different cell lines.

The expression level of the selected wt or mutant CREB expressing clones were further analyzed by immunocytochemistry. Compared to wtPC12 cells the wt or mutant CREB expressing clones showed considerably higher CREB occupancy mostly in euchromatin regions (for Pearson's correlation coefficient see Table 2) indicated by single-layer confocal images using indirect CREB-specific immunocytochemistry (Figure 7). On single-layer confocal images CREB expression levels of the different CREB construct-transfected cell lines showed 2.6-3.7 fold increase compared to wtPC12 cells.

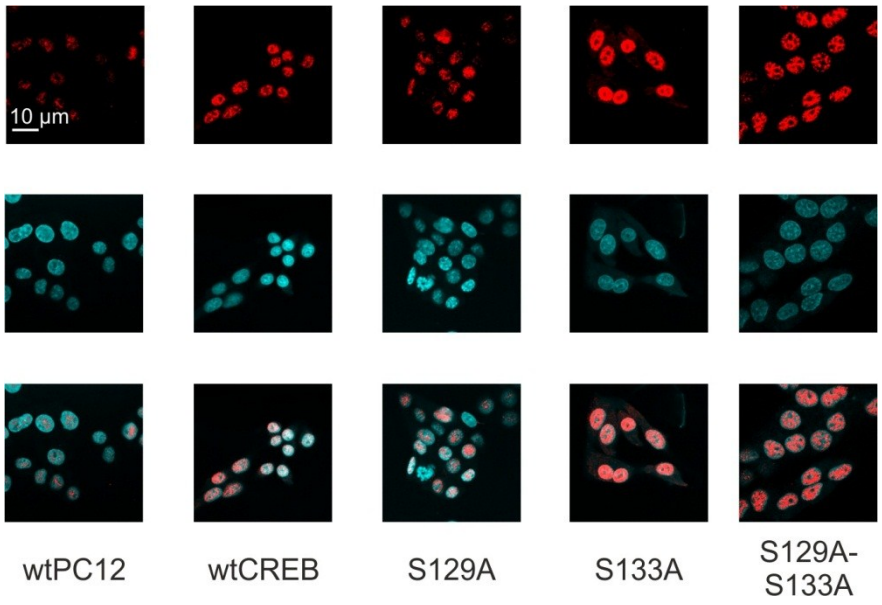

Figure 7 CREB expression in wtPC12 cells and in the various CREB constructs transfected cell lines

Overexpression of wt and mutant CREB increases nuclear CREB occurrence on single-layer confocal images. Red color indicates the presence of CREB protein (top row) using indirect immunocytochemistry, blue color indicates cell nuclei stained by Hoechst 33342 (middle row) and lower row represents merged images. Scale bar denotes 10 µm. The experiment was repeated for three times. A representative result is shown.

Cell line	Pearson's correlation coefficient of the CREB-signal and euchromatin
wtPC12	0.75954
wtCREB overexpressing cells	0.83369
S129A expressing cells	0.75077
S133A expressing cells	0.87473
S129A-S133A expressing cells	0.69144

Table 2 Pearson's correlation coefficient of the Cy3-fluorescent signal according to the CREB protein and euchromatin regions

6.2 CREB decreases the TM-induced apoptosis in PC12 cells

To determine the toxic concentration of TM wtPC12 cells were exposed to different concentrations of the agent for 72 hours and viability of the cells was determined using ATP assay. The concentration resulting in a 50% decrease in viability was found 0.01 μg/ml (referred through the thesis as low concentration TM). The 5 μg/ml concentration of TM (referred through the thesis as high concentration TM) was completely toxic for the cells Figure 8).

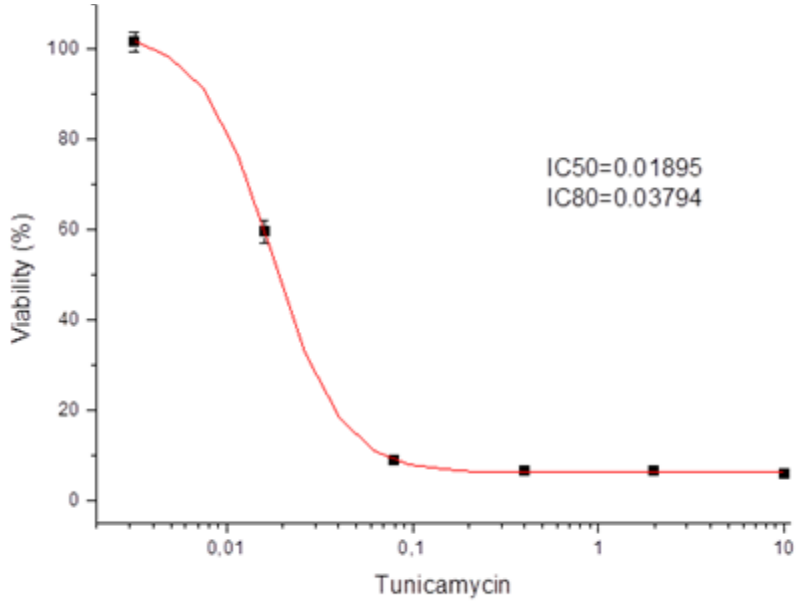

Figure 8 Determination of TM sensitivity of PC12 cells
WtPC12 cells were treated by different concentrations of TM (0.0032, 0.016, 0.08, 0.4, 2, 10 μg/ml) for 72 hours and viability of the cells was determined using ATP assay. IC50 and IC80 values were determined by Origin 8.0 (OriginLab, China).

To determine if CREB overexpression alters TM-induced cytotoxicity ATP assays were conducted using high concentration (5 μg/ml) of TM (Figure 8). WtPC12, wtCREB and mutant CREB expressing cells were treated with TM and assayed for ATP content. The result was normalized to the control activity values of each cell lines. The wt and all mutant CREB overexpressing cells show higher survival rate compared to wtPC12 cells. Survival rate of the S133A-CREB overexpressing cells was statistically different from the wtPC12 results (Figure 9).

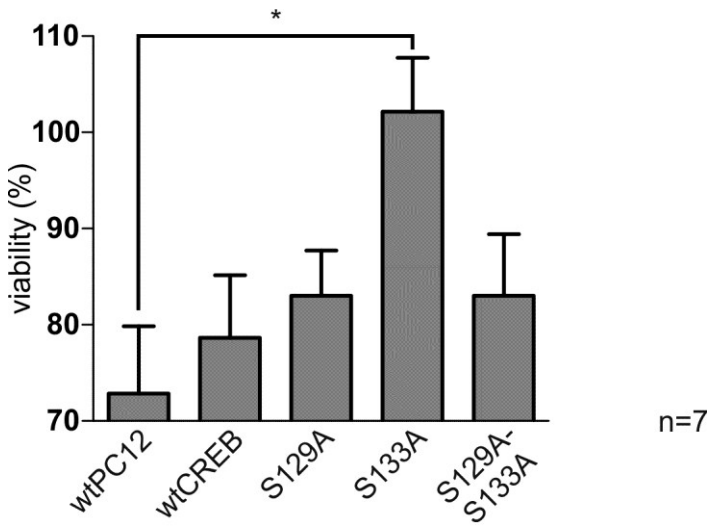

Figure 9 Overexpression of wt and mutant CREB protects PC12 cells from TM induced apoptosis – ATP assay

Comparison of TM cytotoxicity by ATP assay. WtPC12, wtCREB and mutant CREB expressing cell lines were treated with 5 μg/ml TM for 24 hours and ATP assay was performed as described in the Materials and methods. Data were normalized onto control ATP assay activity of each cell line. Figure shows the values of the different cell lines treated by TM. Results of 7 independent experiments are shown. Lines indicate mean ±SEM. One-way ANOVA $P<0.05$. *=$P<0.05$ vs. TM-treated wtPC12.

These results were confirmed by apoptosis assays (Figure 10). Control and TM-treated cells were studied by fluorescence microscopy and apoptotic cells were counted by nuclear morphology after staining with Hoechst 33342 dye. Low concentration of TM did not alter significantly the rate of apoptosis (data not shown). In control samples 5-8% of the cells were apoptotic in both the wtPC12 and the different stably transfectant cultures. High TM concentration induced apoptosis in approximately 35% of wtPC12 cells (Figure 10) during the 24 hour treatment period. In contrast, overexpression of the wtCREB and the S133A mutant CREB rescued cells from apoptosis, in these cultures approximately 15% of cells underwent apoptosis and this result was significantly different form the TM-treated wtPC12 cells. Expression of the S129A-CREB and the double S129A-S133A mutant CREB induced 22 and 23% apoptotic cells, respectively, which result was significantly different from the wtCREB and from the S133A-CREB mutant overexpressing cell lines (Figure 10).
These findings demonstrate that the overexpression of CREB can partially protect cells from TM-induced apoptosis, even if its phosphorylation sites are blocked.

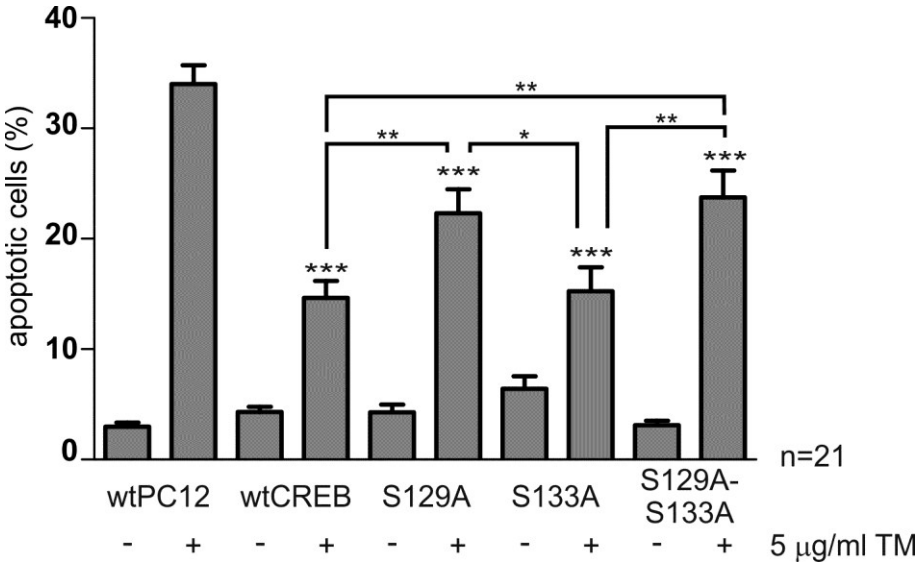

Figure 10 Overexpression of wt and mutant CREB protects PC12 cells from TM induced apoptosis – apoptosis assay

Comparison of TM cytotoxicity by apoptosis assay. TM induces apoptosis in wtPC12 cells which is reduced by the expression of CREB constructs. WtPC12, wtCREB and mutant CREB expressing cell lines were treated with 5 μg/ml TM for 24 hours. Cells were stained by Hoechst 33342 and apoptotic nuclei were counted using a fluorescence microscope. 200-250 cells were counted per sample in randomly chosen viewfields. Apoptotic cells were calculated as a percentage of the total number of cells. Results of 21 independent experiments are shown. Value represents the mean ±SEM. One-way ANOVA $P<0.05$. *=$P<0.05$, **=$P<0.01$, ***=$P<0.001$ vs. TM-treated wtPC12 cells.

6.3 TM provokes ER stress in the different PC12 cell lines

To determine if increased resistance of CREB overexpressing cells towards TM treatment is caused by the absence of triggering endoplasmic reticulum stress the activation of the different main pathways of endoplasmic reticulum stress were checked using Western blotting (Figure 11) and immunocytochemistry (Figure 12) The hallmark of UPR activation is the induction of the chaperon BiP/GRP78 protein; therefore the effectiveness of TM treatment was confirmed. 24 hours of TM treatment increased the amount of BiP protein in wtPC12 and in all types of CREB-transfected cell lines in a dose-dependent manner (Figure 11). Then specific target molecules for each of the three pathways of UPR were chosen. The amount of ATF6 was increased in wtPC12 and in all CREB overexpressing clones in comparison with their untreated control samples. The quantity of tATF6 did not increase in wtPC12 cells; however overexpression of wtCREB decreased the tATF6 level, furthermore

all mutant CREB expressing cell lines showed a slight diminution in the level of tATF6. In wtPC12 cells TM treatment induced the phosphorylation of IRE1 and we observed the same rate of the phosphorylation in all CREB overexpressing cell lines, although the level of phosphorylation was slightly decreased in comparison with the level in wtPC12 cells. The activation of stress kinases JNK and p38MAPK were examined as well. JNK is activated similarly by high concentration of TM in wtPC12 and in the different CREB construct transfected cells. The level of p38MAPK phosphorylation was reduced in the CREB transfected cell lines in comparison to the wtPC12 cells, especially in the wtCREB and in the S133A CREB expressing cell lines. The activation of the PERK arm of ER stress is shown by phospho-PERK dependent eIF2α phosphorylation. As a result of TM treatment, a slightly increased phosphorylation level of the eIF2α protein can be detected in wtPC12, S129A-CREB and S129A-S133A-CREB expressing cell lines. In wtCREB and S133A-CREB expressing cell lines the eIF2α phosphorylation level decreased in comparison with the control samples (Figure 11).

These results confirm that the ER stress response is activated after chronic exposure of TM in wtPC12 and in the different CREB overexpressing cell lines as well, although some components e.g. p38MAPK, eIF2α display slight differences in the subclones.

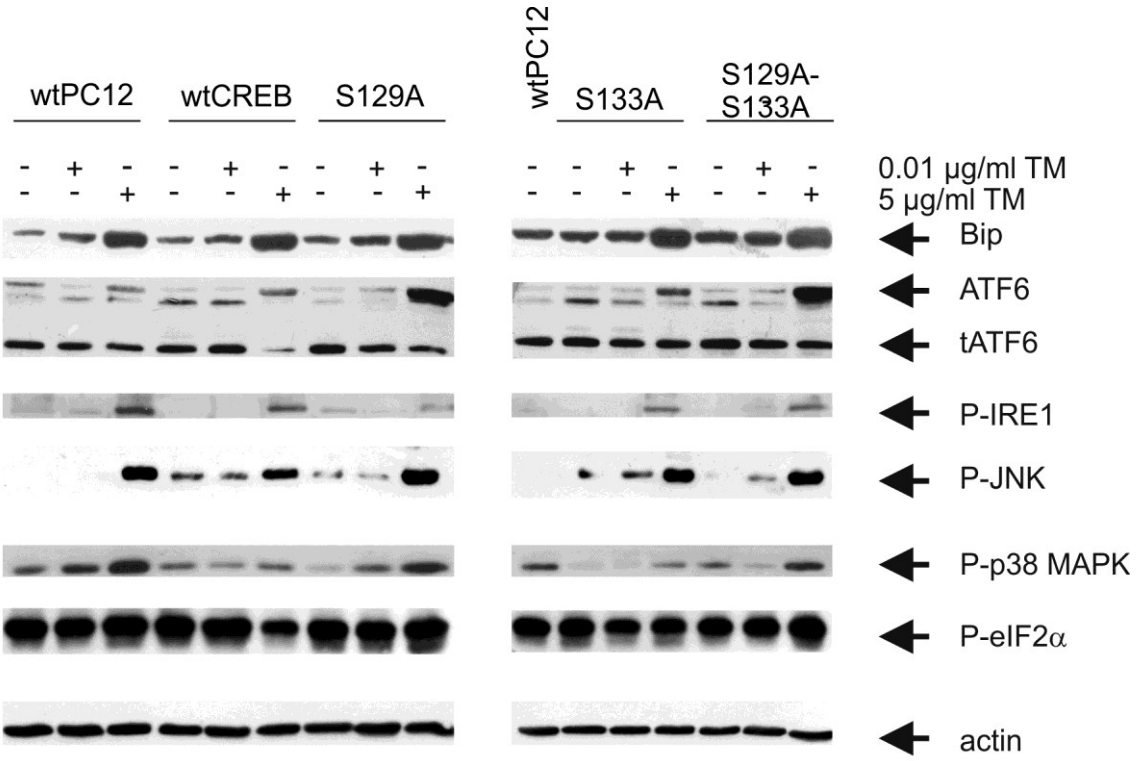

Figure 11 TM-induced ER stress

ER stress is activated after TM treatment in all types of cells. Cells were treated with TM for 24 hours as indicated in the figure and protein expression was analyzed by Western blotting. Actin level was used as a loading control of the protein samples. At least three independent experiments were performed. Representative blots are shown.

Upregulation of the transcription factor CHOP is a common point of convergence in all three pathways of the UPR. Therefore we also examined CHOP induction in the TM-treated cell lines by immunocytochemistry (Figure 12). The induction of CHOP can be detected after TM treatment in wtPC12 and in all CREB-transfected cell lines.

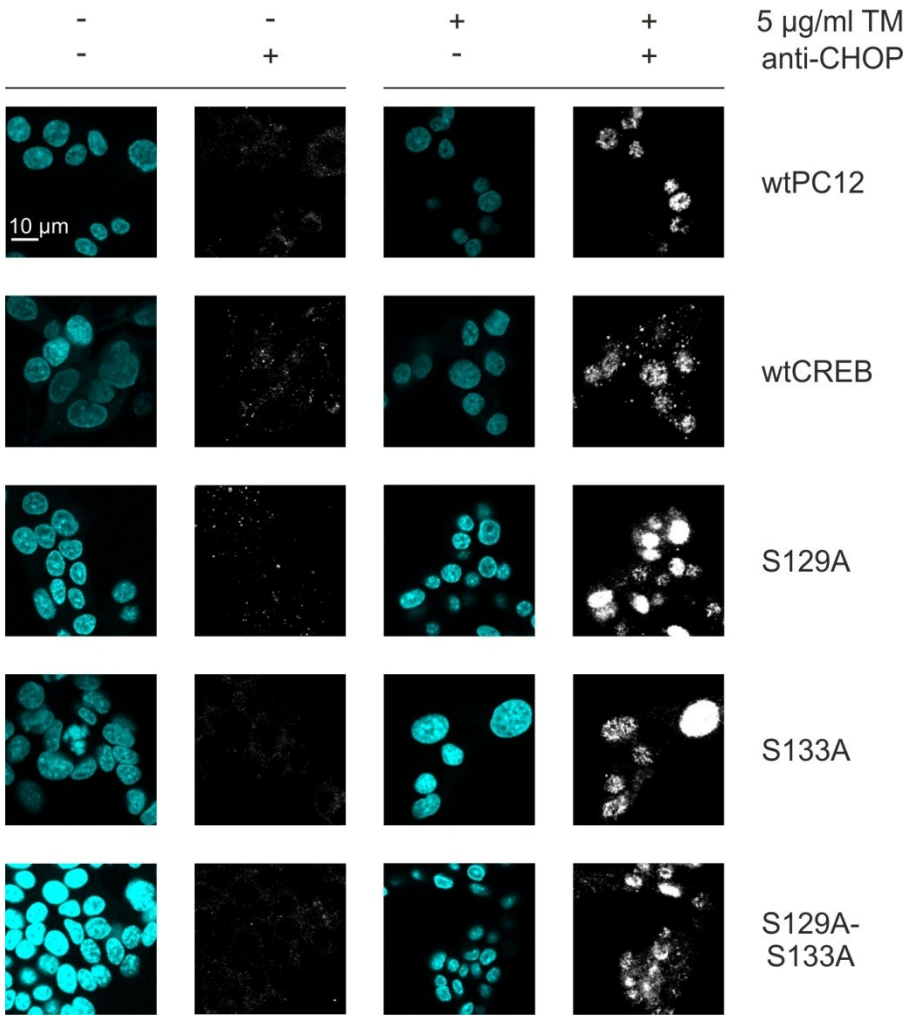

Figure 12 CHOP expression after 24 hours of TM treatment

TM treatment induced CHOP expression in wtPC12 cells and in the CREB constructs expressing cell lines. Expression of CHOP was detected by indirect immunocytochemistry using wtPC12 and CREB overexpressing cell lines on single-layer confocal images as described in the Materials and methods. White color indicates the presence of CHOP protein, blue color indicates cell nuclei stained by Hoechst 33342. Scale bar denotes 10 µm. The experiment was repeated three times. Representative results are shown.

6.4 TM-induced apoptosis can be prevented by the inhibition of GSK-3β

GSK-3 has been described as a mediator of ER stress-induced apoptosis in several different cell types. It was assumed to be essential to confirm if GSK-3 plays a role in the TM-induced apoptosis in the cell lines investigated by using GSK-3 inhibitors, since CREB phosphorylation on residue S129 has been reported to be GSK-3 dependent.

WtPC12 and the different CREB construct expressing cell lines were pre-treated with the widely used inhibitor of GSK-3 LiCl for 60 minutes prior to the 24 hours of TM treatment and cells with apoptotic nuclear morphology were scored in a fluorescence microscope (Figure 13.a). LiCl treatment reduced the TM-induced apoptosis in wtPC12 and in all CREB construct-transfected cell lines. In wtPC12 and in the double mutant S129A-S133A CREB expressing cell lines this inhibition was significant.

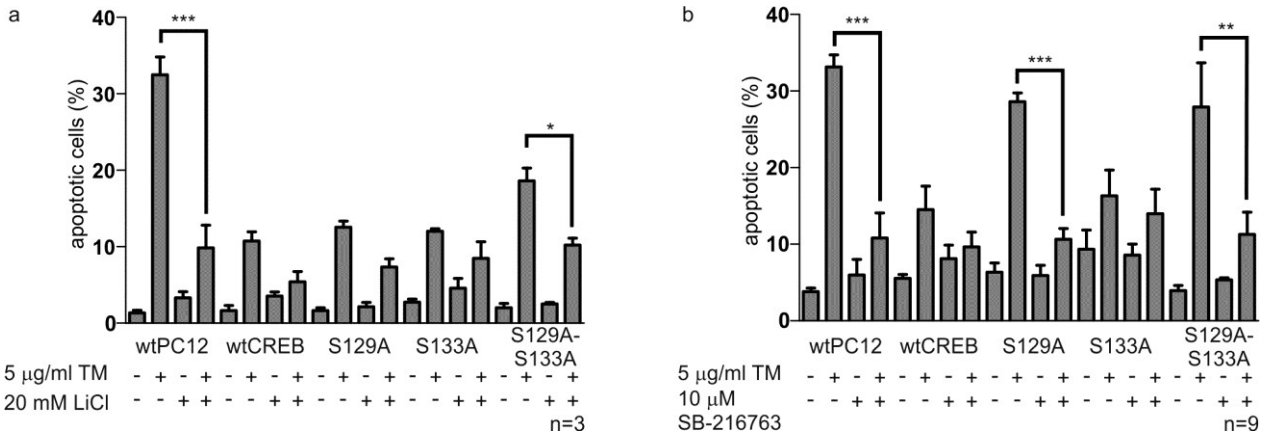

Figure 13 TM-induced apoptosis can be reduced by using GSK-3 inhibitors

a) LiCl treatment decreases the TM-induced apoptosis in wtPC12 and in the CREB overexpressing cells. Cells were treated with TM for 24 hours; in the combination treatment cells were pre-treated with 20 mM LiCl for 60 minutes and afterwards treated with 5 μg/ml TM + 20 mM LiCl for 24 hours. Apoptotic nuclei were scored after staining by Hoechst 33342 in a fluorescence microscope as described in Figure 3. Results of 3 independent experiments are shown. Lines indicate mean ±SEM. One-way ANOVA $P<0.05$. *=$P<0.05$, ***=$P<0.001$.

b) SB-216763 treatment inhibits the TM-induced apoptosis in all cell types. Cells were treated with TM for 24 hours; in the combination treatment cells were pre-treated with 10 μM SB-216763 for 60 minutes and afterwards treated with 5 μg/ml TM + 10 μM SB-216763 for 24 hours. Apoptotic nuclei were scored as described in Fig. 4.a. Results of 9 independent experiments are shown. Lines indicate mean ±SEM. One-way ANOVA $P<0.05$. **=$P<0.01$, ***=$P<0.001$.

Similar results were obtained when another selective GSK-3 inhibitor, SB-216763 was used. Cell lines were pre-treated with SB-216763 for 60 minutes prior to 24-hour TM treatment and apoptotic nuclei were scored in a fluorescence microscope (Figure 13b). As LiCl, the SB-216763 treatment reduced the TM-induced apoptosis in wtPC12 and in all CREB construct-transfected cell lines. In these experiments the decrease in the rate of apoptosis as a result of the inhibition of GSK-3 was significant in the wtPC12, in the S129A CREB and in the

double mutant S129A-S133A CREB expressing cell lines. Inhibition of GSK-3β by LiCl and SB-216763 was confirmed using GSK-3β specific siRNA-mediated knockdown (Figure 14).

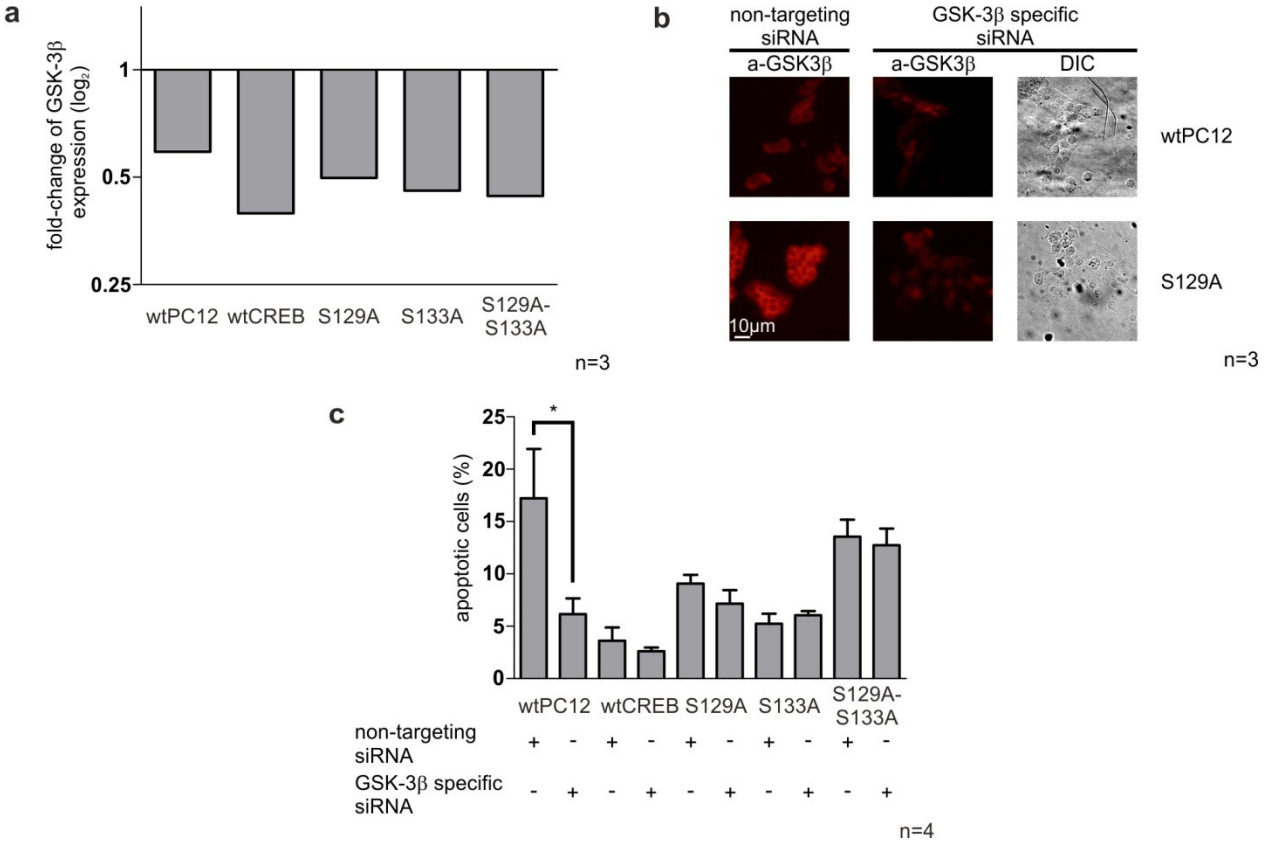

Figure 14 Knockdown of GSK-3β using siRNA technique

a) Validation of GSK-3β knockdown using siRNA technique. Fold-change of GSK-3β expression normalized onto the expression level of 18S compared to non-targeting siRNA samples is shown.
b) Downregulation of GSK-3β confirmed by immunocytochemistry. GSK-3β specific siRNA transfected cells showed 50-75% decrease in fluorescent intensity compared to non-targeting siRNA-transfected samples. Experiments were repeated three times. Representative images are shown.
c) Non-targeting siRNA or GSK-3β-specific siRNA was transfected into different cell lines as indicated on the figure. 72 hours after transfection cells were treated with TM for 24 hours and apoptotic cells were counted. Results of 4 independent experiments are shown. Lines indicate mean ±SEM. One-way ANOVA $P<0.05$. *=$P<0.05$

It is known, that Akt phosphorylation of GSK-3β on serine-9 inhibits its kinase activity. On the other hand Jope et al [98] have demonstrated that the GSK-3 inhibitor LiCl reduces GSK-3 activity directly and by increasing the inhibitory phosphorylation of GSK-3. To examine these effects cells wtPC12 and CREB-transfected cells were treated with LiCl and TM alone

as well as with the combination of both. As it was expected the level of GSK-3β phosphorylation was increased in the LiCl-treated samples in all cell lines. TM treatment induced the activation of GSK-3β in wtPC12 and in all CREB construct expressing cell lines; the level of phosphorylation decreased in comparison with the control samples. LiCl treatment in combination with the TM treatment decreased GSK-3β activity in all cell lines (Figure 15).

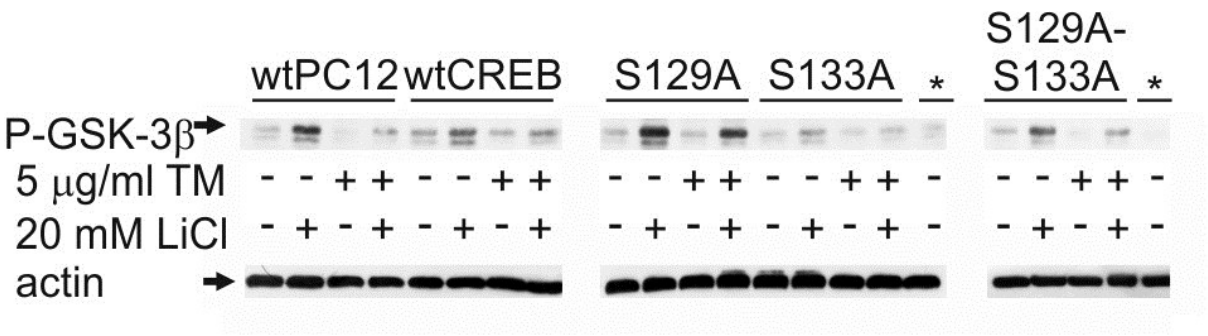

Figure 15 GSK-3β can be inhibited by LiCl pre-treatment
GSK-3 is active in all types of cells after TM treatment. Cells were treated with TM for 24 hours; in the combination treatment cells were pre-treated with 20 mM LiCl for 60 minutes and afterwards treated with 5 μg/ml TM + 20 mM LiCl for 24 hours and Western blot was performed using a phospho-Ser9 specific GSK-3 antibody. Samples with the asterisk are control wtPC12 cell samples. Actin was used as loading control. At least three independent experiments were performed. A representative blot is shown.

To check the phosphorylation state of S129 and S133 residues on CREB protein in PC12 cell lines, Western blot experiments were performed using phospho-CREB-specific antibodies. The phosphorylation of S129 residue on CREB protein was detected in all of the cell lines except in the S129A-S133A CREB double mutant cells. The slight increase in the phosphorylation of the S129A CREB mutant after TM treatment could be caused by the phosphorylation of the endogenous CREB protein. Increased CREB phosphorylation was detected on residue S133 in the wtPC12, in the wtCREB and in the S129A CREB expressing cell lines after TM treatment. In the S133A CREB and in the double mutant S129A-S133A CREB expressing cells the phosphorylation level did not change in comparison to the control samples (Figure 16). The endogenous CREB protein expression level did not change significantly after TM treatment in our PC12 cell lines (Figure 16).

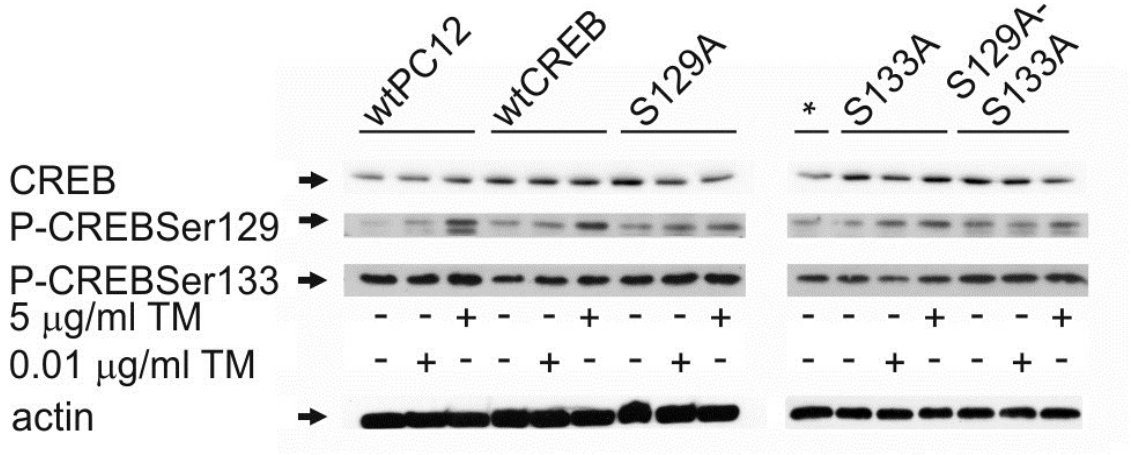

Figure 16 TM treatment induces the phosphorylation of the S129 and S133 residues of CREB protein

Cells were treated with TM as indicated on the figure and Western blot experiment was performed using unphosphorylated and phospho-specific CREB antibodies. Sample with the asterisk is a control wtPC12 cell sample. Actin was used as loading control. At least three independent experiments were performed. A representative blot is shown.

6.5 CREB overexpression alters the expression of Bcl-2 family members

Considering the importance of the Bcl-2 family members in the regulation of ER stress, the involvement of pro- and anti-apoptotic members of the Bcl-2 family was investigated in TM-induced apoptosis. Since the activation of the pro-apoptotic BH3-only family member Bim protein is essential for ER stress-induced apoptosis in several different cell types [99], we wanted to determine the Bim expression in our CREB expressing cell lines. As a result of alternative splicing, there are three splice variants of Bim expressed (Bim-extra-long [Bim_{EL}], Bim-long, [Bim_L] and Bim-short [Bim_S]). Bim_{EL} is the most abundant and it is sequestered on microtubules in a complex with dynein light chain [100]. In wtPC12 cells TM treatment caused a slight increase of Bim_{EL} protein expression, while in the different CREB construct expressing cells the amount of Bim_{EL} decreased as a result of the TM treatment. In the wtCREB and the S133A CREB expressing cells this decrease was pronounced, while the expression of the S129A-CREB and the S129A-S133A-CREB was associated with a modest decrease in Bim_{EL} expression. The Bim_L and Bim_S levels showed increased expression of these splice variants after 24 hours of high concentration of TM treatment in wtPC12 cells and the level of both of them decreased in all CREB

overexpressing clones (Figure 17). As Bim has been shown to interact with other members of the Bcl-2 protein family, including Bcl-2, Bcl-X_L, and Mcl-1 [101], we examined the level of those proteins after TM treatment. The expression of the Bcl-2 protein decreased in wtPC12 cells and in all CREB overexpressing cell lines. In the wtCREB and in the S133A CREB expressing cells a marked decrease was observable in the control samples in comparison to the wtPC12 and the other mutant CREB expressing cells (Figure 17). These results confirm previous reports that GSK-3 downregulates CREB by phosphorylating the S129 residue, therefore the expression level of proteins depending on CREB transcriptional activity are decreased. The expression of Mcl-1 decreased in wtPC12, in wtCREB and in the S133A CREB expressing cells as a result of the TM treatment. The Bcl-X_L and Bcl-w level showed a slight decrease only in the S133A CREB expressing cells (Figure 17).

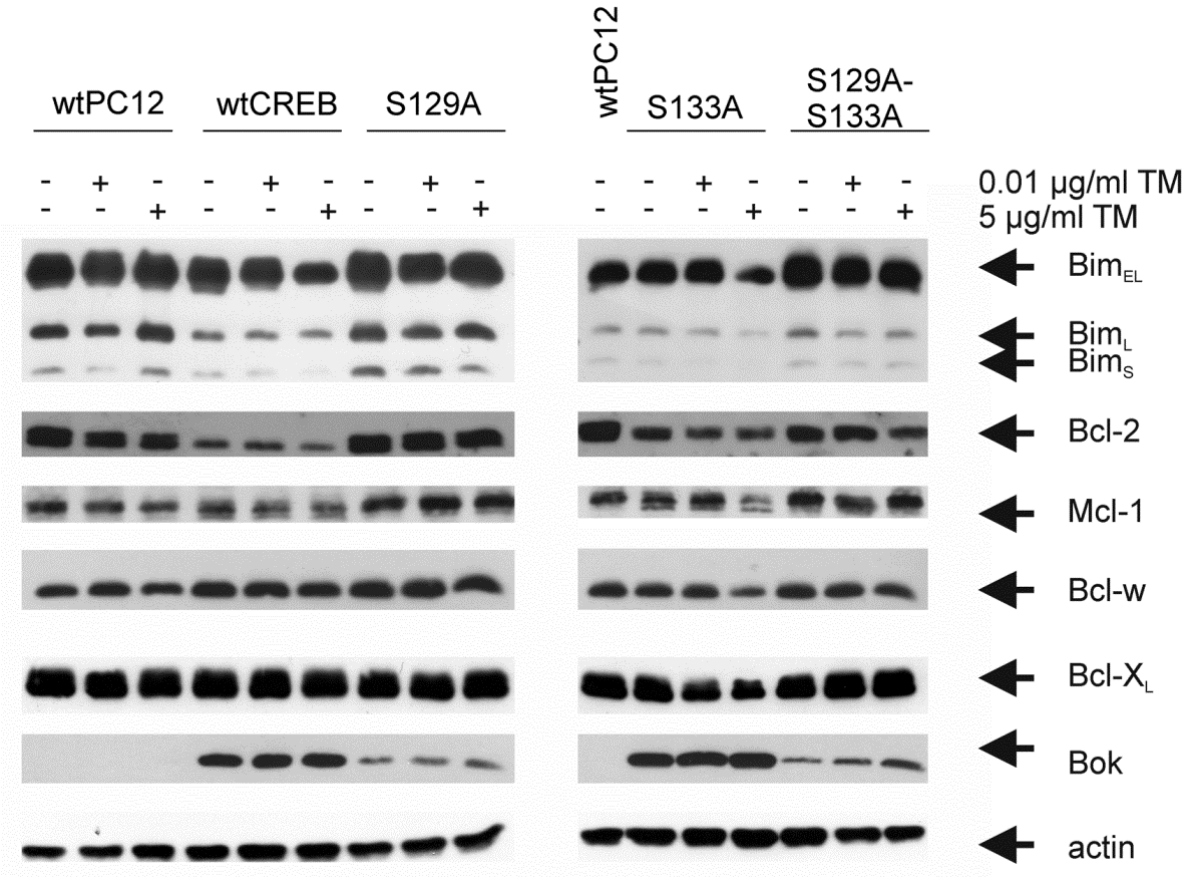

Figure 17 The effect of TM treatment on the expression of Bcl-2 family members
Cells were treated with TM for 24 hours as indicated in the figure and protein expression was analyzed by Western blotting. Actin was used as a loading control. At least three independent experiments were performed. Representative blots are shown.

Bok is a ubiquitously expressed member of the pro-apoptotic multidomain Bcl-2 family, which activates the intrinsic apoptosis pathway [102]. In wtPC12 cells TM induced the Bok expression up to 10 hours and it was completely abolished by 24 hour (Figure 18). Interestingly, the expressions were very strong in the wtCREB and in the S133A CREB control cells and no significant change could be detected in the level of expression even after 24 hours of TM treatment (Figure 17). In S129A and S129A-S133A CREB expressing cells the Bok expression was lower in the control samples and a slight increase can be detected due to TM treatment (Figure 17).

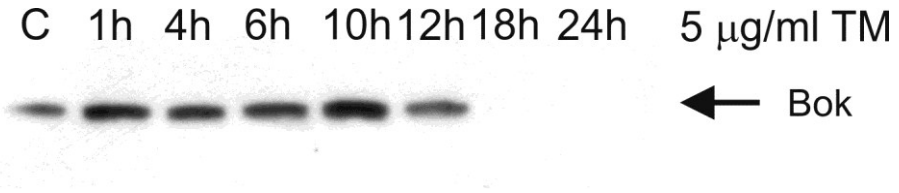

Figure 18 The effect of TM treatment on the expression of Bok
WtPC12 cells were treated by high concentration of TM for 1, 4, 6, 10, 12, 18 and 24 hours and a Western blot experiment was performed.

6.6 CREB influences the association of Bim to the microtubule network

Bim has been reported to bind to the actin and microtubule cytoskeletal network in resting cells [103]. Upon different stress stimuli JNK and p38 MAPK stress kinases are able to induce dissociation of Bim from the cytoskeleton and activate the intrinsic pathway of apoptosis. Fluorescence resonance energy transfer (FRET) in confocal microscopy was used to characterize the interaction between Bim and the microtubule network. Since Bim does not directly bind to the cytoskeleton, but for instance binds through the dynein complex to the microtubule system, indirect labeling was aimed to be strong enough to study energy transfer between the labeled Bim and tubulin molecules. For the energy transfer acceptor photobleach method was used with Cy3-labeled rabbit anti-rat specific antibody as a donor and donkey Cy5-labeled anti-mouse antibody as the acceptor recognizing Bim and β-tubulin, respectively. Between taking the pre-bleach and post-bleach images, area of interest was photobleached and the whole picture was obtained for FRET analysis. Energy transfer could be detected between these two fluorophores with R_0=5.1 nm Förster

distance. In control cells a clear association of Bim and the microtubule labeling could be observed (Figure 19). In wtPC12 cells high concentration of TM treatment induced the diminution of FRET between the fluorophores indicating the separation of Bim from the microtubule complex. In wtCREB overexpressing and CREB mutant expressing cell lines the FRET could be evoked after 24 hours of TM treatment in the cells representing the close localization of the two fluorophores, implicating the association of Bim to the microtubule complex (Figure 19).

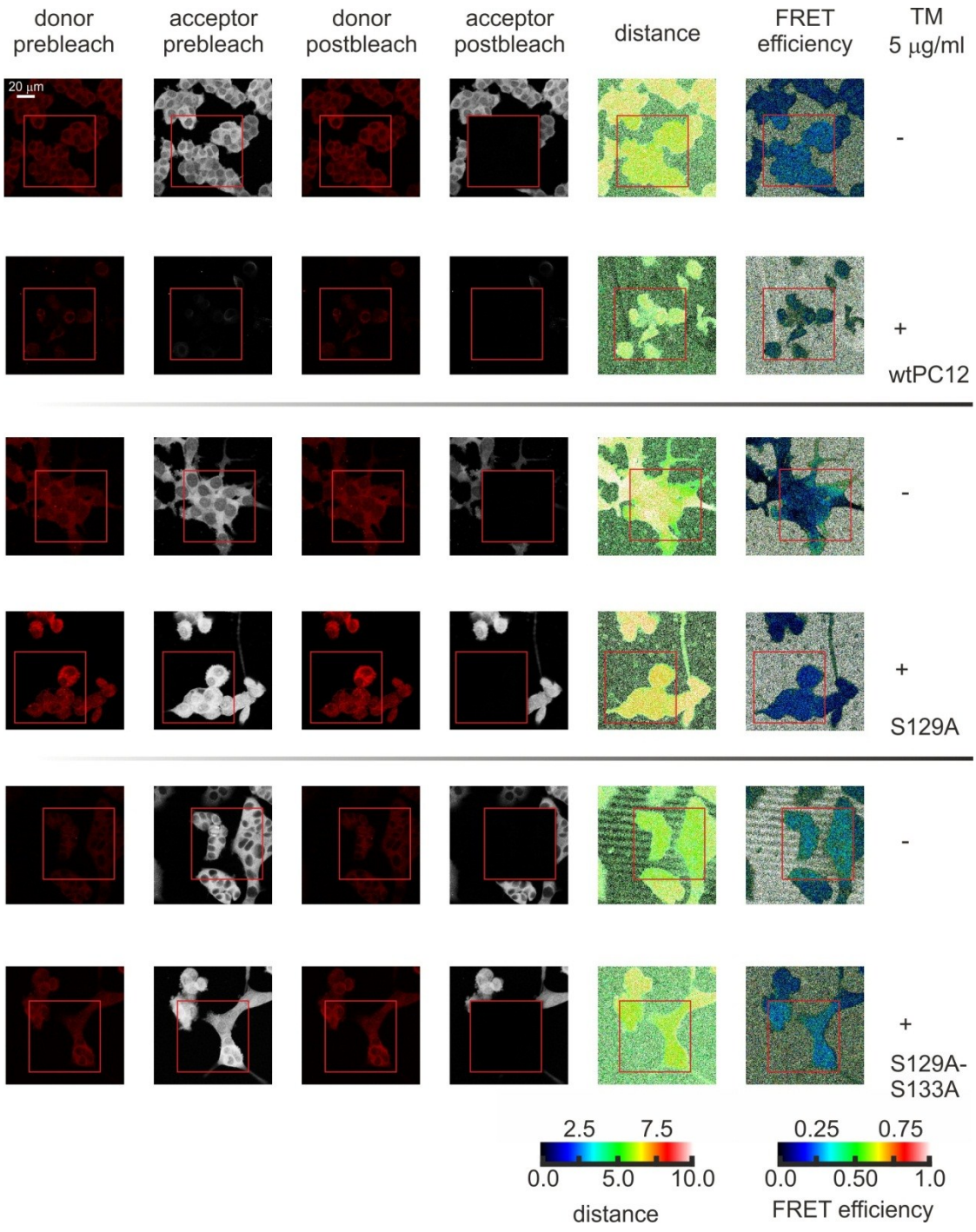

Figure 19 Association of Bim to the microtubule network demonstrated by FRET analysis
Control cells and high concentration TM treated cells were obtained for indirect immunocytochemistry and FRET analysis using Cy3-labeling referring to Bim (red) as donor and Cy5-labeling referring to tubulin (white) as acceptor using acceptor photobleach method. Area of interest was photobleached indicated by the red square and whole images were analyzed determining FRET distance and FRET efficiency. Figure shows a representative result using the S129A CREB clone. All other CREB expressing cell lines showed similar results. Scale bar denotes 20 μm.

6.7 CREB decreases the TM-induced apoptosis in various types of rat cells

WtPC12, Rat-1 and primary RVSM cells were transiently transfected with pcDNA3 and pEGFP-C1 constructs (mock-transfected) or with pcDNA3-CREB and pEGFP-C1 constructs (CREB-transfected). 48 hours after transfection cells were treated with TM or pre-treated with LiCl prior to the 24 hours of TM treatment. Transfected, EGFP positive cells (Figure 6) were scored for apoptosis according to their nuclear morphology in a fluorescence microscope (Figure 5). Overexpression of CREB significantly decreased the TM-induced apoptosis in wtPC12 and in Rat-1 in comparison to the mock-transfected samples. LiCl decreased the cytotoxicity of TM in primary RVSM cells. Parallel to LiCl transient overexpression of CREB clearly reduced TM-evoked apoptosis in wtPC12, Rat-1 and in primary RVSM cells (Figure 20).

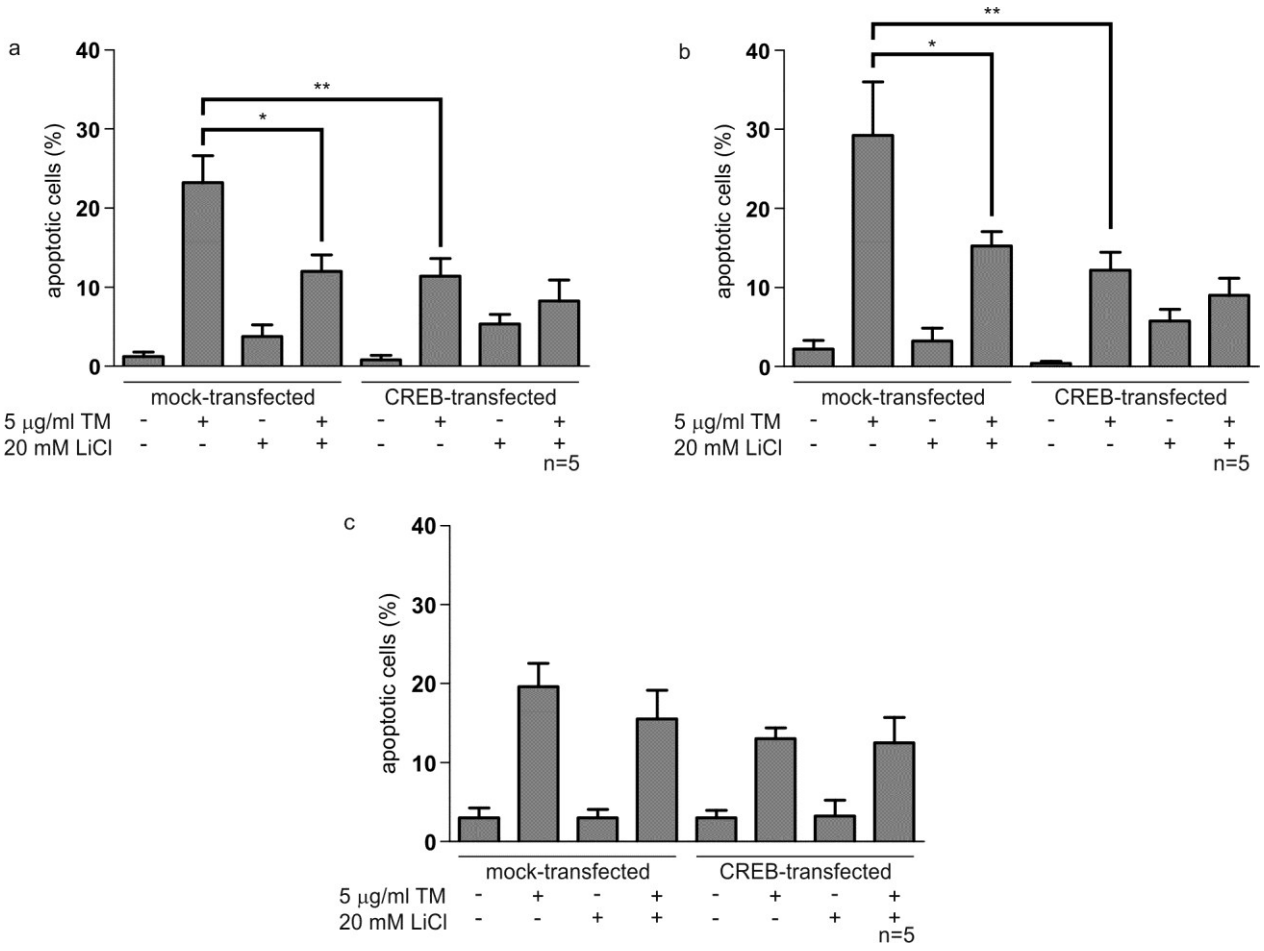

Figure 20 Transient overexpression of CREB and LiCl treatment reduce TM-induced apoptosis in wtPC12 cells, in Rat-1 and in primary RVSM cells

WtPC12 cells (a), Rat-1 cells (b) and primary RVSM cells (c) were transiently transfected with pcDNA3 and pEGFP-C1 vectors (mock-transfected) or pcDNA3-CREB and pEGFP-C1 vectors (CREB-transfected). Cells were treated with TM or LiCl for 24 hours; in the combination treatment cells were pre-treated with 20 mM LiCl for 30 minutes and then treated with 5 μg/ml TM + 20 mM LiCl for 24 hours. Samples were processed for apoptosis assay as described in the appropriate section of Materials and methods. Nuclear morphology of EGFP positive cells was examined and apoptotic nuclei were scored after staining by Hoechst 33342 in a fluorescence microscope as described in Figure 3. Results of 5 independent experiments are shown. Lines indicate mean ±SEM. One-way ANOVA $P<0.05$. *=$P<0.05$, **=$P<0.01$.

6.8 Gene expression alterations in wtPC12 cells after MTH-68/H infection

In order to analyze genome-wide gene expression changes caused by an oncolytic NDV strain in a tumor cell line, total RNA was isolated from uninfected wtPC12 cells and from cultures infected with MTH-68/H for 12 hours at a multiplicity of infection corresponding to the IC_{50} value. Under these conditions PC12 cells develop morphological and biochemical signs of apoptosis and 50% of them die by 72 hours post-infection [85]. The RNA samples were subjected to transcriptional profiling as described in the section 5.13. 729 genes (corresponding to 773 exons) were found to be induced and 612 genes (631 exons) to be repressed by virus-infection, at least two-fold. Transcriptional regulation of 5 of the up-regulated genes (*Ifnb1, Stat2, Casp12, Ddx58* and *Tnf*) and 4 of the down-regulated genes (*Bmyc, Mrpl34, Pole2, Cdc26*) were validated by qRT-PCR (Figure 21). Although with quantitative differences the tendency of regulation by MTH-68/H was found similar using the two different experimental approaches.

Genes with altered expression were categorized into clusters by the DAVID functional annotation clustering tool [104]. The up- and down-regulated genes were classified into 176 and 146 overlapping clusters, respectively.

According to the functional annotation the following pathways were identified from the functional clusters formed.

1. Pathways for innate immunity
    a. RIG-I-like receptor signaling pathways
    b. Toll-like receptor signaling pathways
    c. Interferon-stimulated pathways
2. Pathways of growth factor signaling and cell cycle regulation
3. Pathways of cellular stress and apoptosis
    a. Intrinsic apoptosis pathway
    b. Extrinsic apoptosis pathway
    c. ER stress pathway

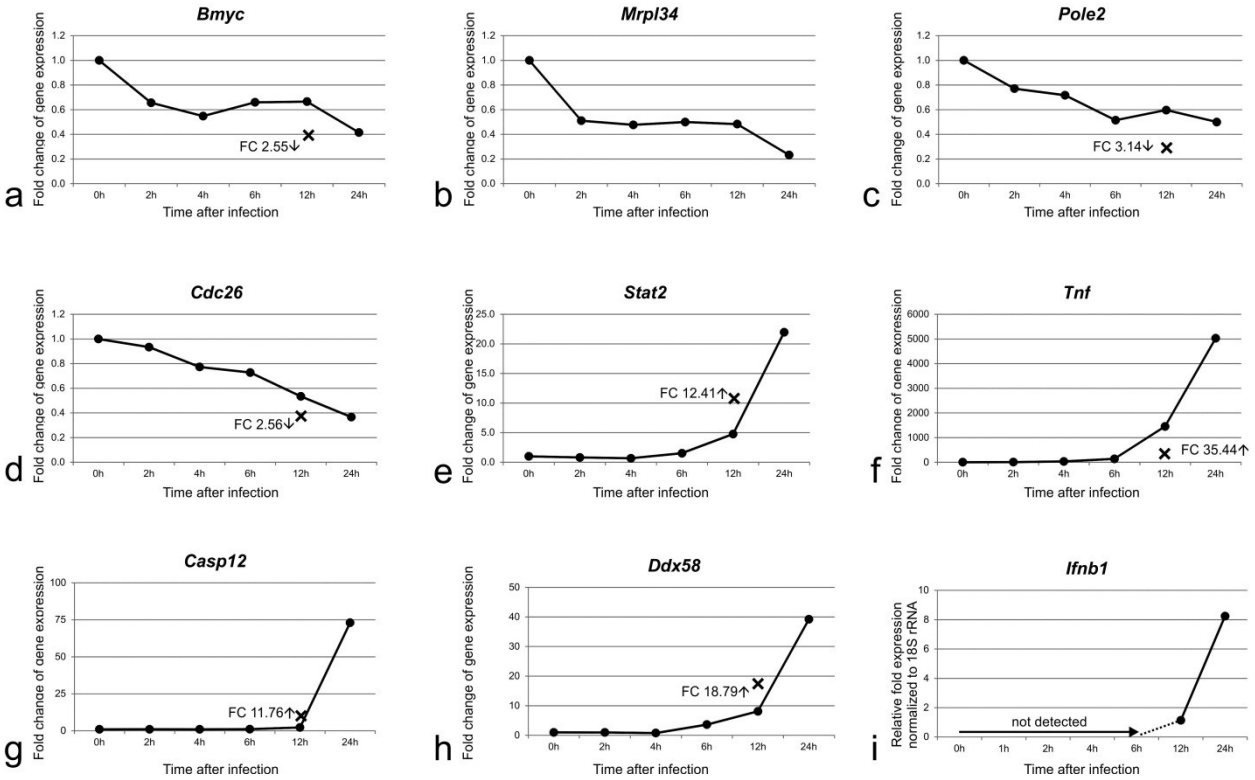

Figure 21 Quantitative reverse transcriptase PCR validation of microarray-based gene expression profiling.

Cells were infected with MTH-68/H at IC50 concentration for the indicated time periods followed by RNA isolation and reverse transcriptase quantitative real time PCR. Charts a to h: gene expressions are expressed as fold-changes of the control value; chart i: gene expression was not detected in uninfected cells, gene expression is represented as relative expression normalized to 18S rRNA. The mark " ✕" and FC values represents the fold-change of gene expression by the microarray analysis.

7 Discussion

7.1 The role of GSK-3β in ER stress

The accumulation of unfolded proteins can initiate ER stress response which can lead to the activation of the apoptotic signaling cascade. The role of this process has been identified in a number of neurodegenerative conditions, in diabetes, in tumor formation, atherosclerosis and in aging.

In the last several years, GSK-3β has been proved to be an important modulator of apoptosis and ER stress. Activation of GSK-3β is linked directly to increased neuronal apoptosis and seems to play a significant role in Alzheimer's disease and in other degenerative disorders as well as in cancer. Revealing and characterizing the role of GSK-3β in the signal transduction of the ER stress is essential to develop rational therapy of these conditions.

There are multiple mechanisms that can regulate the inactivation of GSK-3β via Ser-9 phosphorylation, among those the PI 3-K/Akt pathway is one of the best characterized cell survival signaling pathways. GSK-3β regulates its downstream targets, among them a number of transcription factors directly through phosphorylation [105], one of them is the nuclear phosphoprotein CREB. The mechanism by which ER stress activates GSK-3β activity is not completely clear. Song et al. [42] reported that ER stress signaling induces the protein phosphatase 2A-dependent dephosphorylation of GSK-3β, and the subsequent GSK-3β-dependent induction of apoptosis in human SH-SY5Y neuroblastoma cells (Figure 1).

Several papers have been published proving the anti-apoptotic function of CREB: CREB null mice expressing functionally inactive CREB die immediately after birth [106], human melanoma cells expressing a dominant-negative CREB mutant had increased susceptibility to TG-induced apoptosis [107], inhibition of CREB activation promotes apoptosis [108], CREB blocks okadaic acid-induced apoptosis in PC12 cells [109].

PC12 cell line isolated in 1976 by Greene and Tischler [110] is a widely-used model system to study neuronal development, differentiation, apoptosis and ER stress. Hiroi et al. showed that LiCl has a protective effect in PC12 cells against TG-induced ER stress [111]. Takadera et al. demonstrated that inhibition of GSK-3 by GSK-3 specific ATP-competitors SB-216763,

azakenpaullone and alsteropaullone protects PC12 cells and rat cortical neurons from TG-induced apoptosis [112, 113]. Brefeldin A (BFA) was characterized to inhibit anterograde vesicular transport and secretion in PC12 cells [114-116]. In PC12 cells and in several other cell lines the prolonged exposure of BFA results in the perturbation of the Golgi-complex and induces ER stress leading to apoptosis [117]. Eleyaman et al. [118] demonstrated that the GSK-3 inhibitor LiCl can rescue cortical neurons from BFA-induced cell death. Kögel et al. found that wt human amyloid precursor protein has neuroprotective effect on PC12 cells and inhibits apoptosis evoked by TM and BFA [119]. Moreover, PC12 cells were shown to be rescued from TM-induced, but not TG-evoked cell death by nicotine [120, 121].

7.2 The significance of S129 and S133 residues of CREB in the ER stress

The three arms of ER stress signaling were stimulated during prolonged TM treatment in the PC12 cell lines used. Increase in the level of chaperon BiP was observed in all cell types indicating the propagation of induced adaptation mechanisms (Figure 11). The level of the tATF6 showed decrease, meanwhile a prominent rise of the full length uncleaved ATF6 could be observed in the S129A and S129A-S133A double mutant clones. Triggering of the IRE1 pathway and subsequent activation of the stress kinases JNK and p38 MAPK was evoked in all cell lines. PERK-dependent attenuation of the global translation by the phosphorylation of eIF2α was decreased in wtCREB and in S133A cell lines (Figure 11). The ATF4/ATF6-dependent CHOP expression could be detected in the nuclei of all cell types, which clearly indicates the active ER stress response (Figure 12).

Although ER stress was evoked, the present study shows that wt and different phosphorylation site mutant CREB proteins were able to protect PC12 cells from TM-induced apoptosis (Figure 9, Figure 10). Different mechanisms can be considered to be responsible for the increased survival of these cell lines (Figure 22).

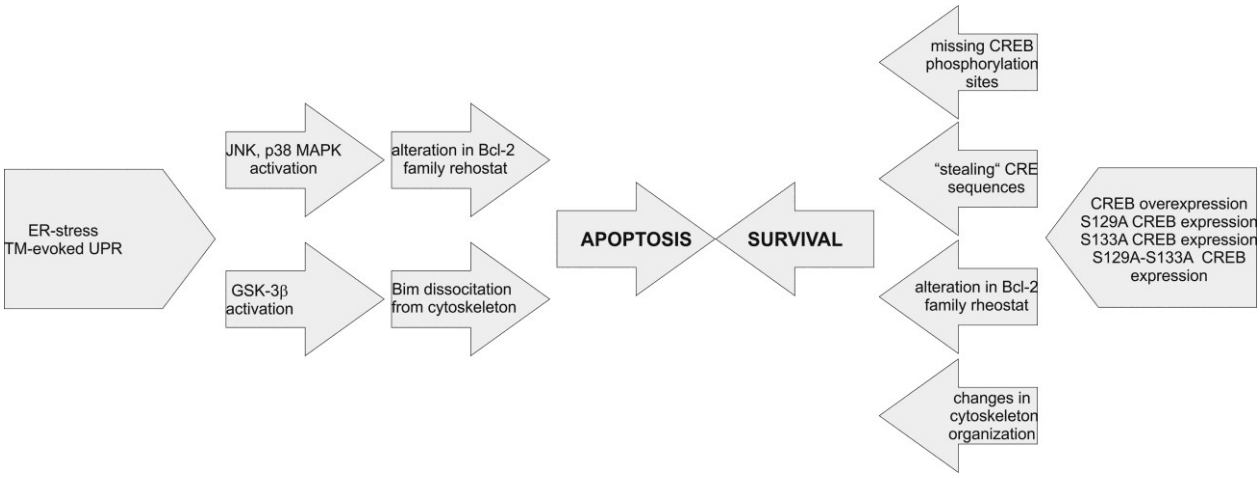

Figure 22 Possible mechanisms determining survival of wtCREB overexpressing and mutant CREB expressing cell lines.

One possible explanation for the increased cell survival is the absence of S129 and/or S133 phosphorylation sites. It was demonstrated that GSK-3β has a central role in the ER stress signaling pathway in our cell lines, since inhibitors of GSK-3β (LiCl and SB-216763) partially protected PC12 cells from TM-induced apoptosis (Figure 13).

CREB activity is regulated by numerous kinases through complex phosphorylation mechanisms that are not completely characterized. Gonzalez and Montminy [122] discovered that phosphorylation of CREB at S133 is required for CREB to be transcriptionally active.

Wang et al. [123] further demonstrated that phosphorylation of CREB at S133 created a consensus site for phosphorylation by GSK-3β at S129. Few studies have addressed the functional consequences of this secondary phosphorylation of CREB by GSK-3β.

Fiol et al. [46] provided evidence that GSK-3β facilitated activation of CREB. In contrast, others found that phosphorylation of CREB by GSK-3β attenuated PKA-induced CREB DNA binding activity [47]. Grimes and Jope [35] found that CREB activity was inversely related to GSK-3β activity in SH-SY5Y cells subjected to a number of treatments, and that overexpression of GSK-3β greatly attenuated the activity of CREB. Moreover, Ozaki and Chuang [124] reported results consistent with an inhibitory effect of GSK-3β on CREB activity that lithium treatment increased CREB DNA binding activity. The binding of the co-activator protein CBP was stimulated by inhibition of GSK-3β, indicating that inhibition of

GSK-3β was sufficient to increase the transcriptional activity of CREB in quiescent cells [125].

GSK-3β phosphorylates CREB protein on S129 during TM-induced ER stress (Figure 16). As this phosphorylation was reported to decrease the DNA binding activity of CREB, this could lead to the decreased expression of the CREB-regulated genes (e.g. Bcl-2). Using computational analysis several thousand genes were found to be CRE-dependent [126, 127] Assuming that GSK-3-dependent CREB phosphorylation highly regulates cell death in PC12 cells, hypothetically the S129 mutants, the S133 mutant cell lines, just like the S129-S133 double mutant cells should show lower apoptotic response to TM, which was confirmed by apoptosis assay experiments (Figure 10).

Another mechanism which could contribute to CREB-dependent survival of these cell lines is the "stealing" of CRE sequences by CREB from ATF6 and ATF4 (Figure 1, Figure 22). CREB has been reported to constitutively bind to its target sequences in both unstimulated and stimulated cells [128]. Cotransfection experiments showed that CREB inhibits the CRE binding ability of ATF4 [129] in vitro. Overexpression of wt and all the mutant CREB proteins decreased the expression of ATF4 in control cells in comparison to the wtPC12 cells. TM treatment induced the expression of ATF4 protein but it did not colocalize with the CREB protein in the CREB expressing clones (data not shown). Previously it was reported that ATF6 interferes with CREB's DNA binding activity on PEPCK and G6Pase promoters [130]. Furthermore it was observed that ATF6 binds to the CREB Regulated Transcription Coactivator 2 (CRTC2) and suggested that it competes with CREB and suppresses its function [131]. The increased attendance of either wt or mutant CREB could interfere with ATF4 and ATF6 transcription factors and could account for the increased survival rate by competing with the apoptosis-inducing ATF6 and ATF4 proteins for CRE, regardless of the presence or phosphorylation state of S129 and S133 sites on the CREB protein.

7.3 The association of CREB and the Bcl-2 family rheostat

Alterations in the expression of the different anti-apoptotic Bcl-2 members were also observed in wtCREB overexpressing and mutant CREB expressing cell lines after TM treatment, which could account for the increased survival of these cell lines. Interestingly, wtCREB overexpressing cells show a reduced amount of Bcl-2, even though several groups identified Bcl-2 expression to be CREB-dependent [132-134] in different models. Cells were preincubated in low serum containing medium for 24 hours and treated with TM for 24 hours as well in low serum containing medium throughout the experiments, GSK-3β assumed to be subsequently active and able to phosphorylate the S129 residue on CREB which leads to decreased Bcl-2 expression. In those cell lines in which the S129 residue is intact on CREB protein (wtCREB and S133A CREB clones) Bcl-2 expression is much weaker compared to wtPC12 cells.

Using a computational approach Impey et al. showed [127] that the *bok* promoter contains a half site CRE sequence, although CREB binding in SACO (serial analysis of chromatin occupancy) library was not confirmed. This could answer the enhanced level of the proapoptotic Bok in CREB overexpressing and mutant CREB expressing cells, however, the TM-induced survival of these cell lines is better compared to wtPC12 cells. Bok selectively binds to the Mcl-1 protein but not to Bcl-2 or Bcl-X_L [135, 136] and Maurer et al. showed that Mcl-1 can be degraded either through ubiquitination after its phosphorylation by GSK-3 [137] or by an ubiquitin-independent mechanism [138] (Figure 23). Increased Bok expression in wtCREB and S133A CREB expressing cells might contribute to the sequestration of Mcl-1 after TM treatment as it can be seen in Figure 23. According to our experiments expression of different CREB constructs prolongs the expression of Bok protein since in wtPC12 cells it is not expressed after 24 hours (Figure 23). The presence of S129 residue in the CREB protein enhances the level of its expression. Bok expression did not change significantly after TM treatment of the different clones (Figure 23).

The BH3-only Bcl-2 family member Bim is expressed as three splice variants, Bim_{EL}, Bim_L and Bim_S. Translated Bim variants can undergo posttranslational modifications, enhancing or inhibiting the proapoptotic activity of Bim. Harada et al. reported growth factor-dependent suppression of *bim* gene transcription [139]. Bim_{EL} and Bim_L have been reported to be sequestered to dynein light chain in resting cells [99, 103]. All three splice variants are

reported to be able to bind to anti-apoptotic Bcl-2 family members [140, 141] blocking their function and promote cell death [142]. JNK and p38 MAPK have been reported to regulate both ubiquitin-dependent degradation [143-146] and dissociation of Bim from the dynein-light chain complex [103, 147] (Figure 23).

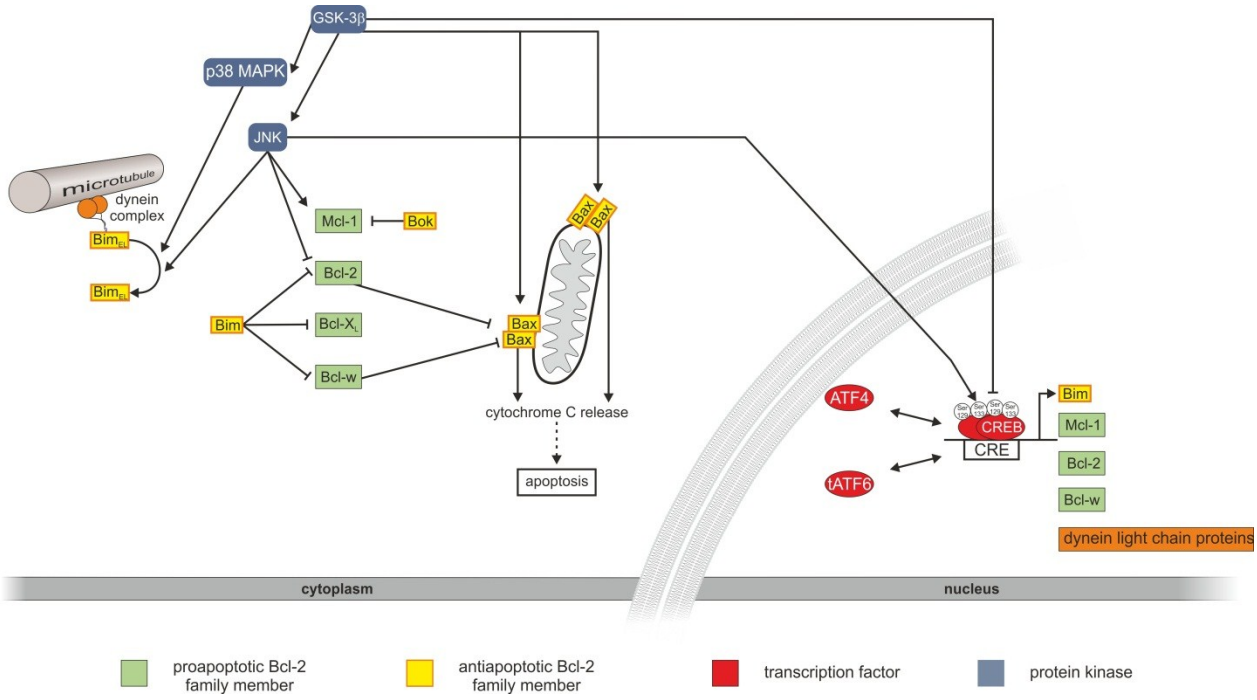

Figure 23 The effect of GSK-3β, JNK and p38 MAPK on the Bcl-2 family rheostat.

7.4 CREB-dependent cytoskeletal rearrangement

Alteration of the cytoskeletal system might also be responsible for the enhanced survival of the CREB expressing cell lines (Figure 22, Figure 23). It was demonstrated by FRET analysis that Bim is located in the vicinity of the tubulin complex under resting conditions (Figure 19) and, as a result of TM-induced ER stress, this association visibly diminished in wtPC12 cells (Figure 19). In wtCREB and mutant CREB expressing cell lines the interaction remained stable even after prolonged ER stress evoked by TM (Figure 19). This phenomenon is clearly indicated on Figure 19 by the color-change of the regions photobleached on the "distance" and "FRET efficiency" images. Association of Bim to the microtubule network allows fluorescence energy transfer between the fluorophores coupled to Bim and β-tubulin molecules appearing as change

of color in the photobleached area compared to the color of the non-photobleached regions. These results could explain the TM-induced high apoptosis rate observed in wtPC12 cells and the decreased cell death in the different CREB expressing cell lines (Figure 9, Figure 10). It is not clear whether this observation is the cause or the consequence of the survival of these cell lines.

Compared to wtPC12 cells all the other cell lines showed a remarkable lower level of the active P-p38 MAPK, nevertheless lower level of active P-JNK level was detected in wtCREB overexpressing cells. Lower activity of these stress kinases could account for decreased phosphorylation of Bim and prolong its binding to the microtubule complex interfering with apoptosis.

Bim_S with its shortest lifespan out of all three splice variants is synthesized upon different stress stimuli *de novo* [148] and possesses the most toxic effect [142]. Wt and S133A CREB cells show noticeably lower Bim_{EL} and Bim_S expression in response to high concentration of TM compared to the other cell lines, which observation can be parallel to the improved survival rate of these cell lines.

Increased survival of wt and mutant CREB expressing cells could be interpreted by the altered Bim rheostat which might be affected at different levels.

It is also possible that CREB regulates cytoskeletal rearrangement since the *Dynll1* gene (encodes for cytoplasmic dynein light chain 1; LC8) and dynein-related genes *Dnch2*-dynein, cytoplasmic, heavy polypeptide 2, *Dnch1*- dynein, cytoplasmic, heavy chain 1, Dncli-dynein, cytoplasmic, light intermediate chain 1, *km23*- dynein-associated protein *RKM23*-dynein-associated protein RKM23, *Dnai2*-dynein, axonemal, intermediate polypeptide 2, *Dncic1*- dynein, cytoplasmic, intermediate chain 1, *Dncli2*-LIC-2 dynein light intermediate chain 53/55, *Pin*- dynein, cytoplasmic, light peptide, *Dncic2*- dynein, cytoplasmic, intermediate polypeptide 2, *Dlc2*- dynein light chain-2) contain CRE promoter regions [127]. PC12 cells transfected with different CREB constructs are larger and attach more firmly to the surface of tissue culture plates (especially the wtCREB and S133A CREB constructs transfected cells) than wtPC12 cells.

7.5 General aspects of the GSK-3β/CREB axis; overexpression of CREB decreases the toxicity of TM in Rat-1, wtPC12 and RVSM cells

Previous studies demonstrated the principal role of GSK-3β and CREB in the survival of Rat-1, PC12 and RVSM cells [39, 44, 109, 149-154]. Transient transfection experiments indicated that overexpression of CREB may potentiate the survival of different cell types used in the present study under prolonged ER stress (Figure 20). As cells were cultured in low serum containing media during transient CREB-expression experiments a remarkable cell loss was observed within 36 hours in the primary RVSM culture (data not shown). Due to this observation the TM-treatment protocol was modified and wtPC12, Rat-1 and RVSM cells were cultured and treated in high serum containing media. Despite of the high serum conditions TM was able to evoke apoptosis in all three cell lines investigated, but interestingly the primary RVSM cells showed the lowest vulnerability towards TM among the cells investigated. This phenomenon might be explained by the high level of growth factors being present in the culture medium of primary RVSM cells, likely to stimulate the growth factor-dependent PI 3-K/Akt pathway leading to the subsequent inactivation of GSK-3β.

7.6 MTH-68/H induces innate immune response and cell death in wtPC12 cells

WtPC12 cells were infected with the oncolytic MTH-68/H attenuated NDV strain. WtPC12 cells are moderately sensitive to MTH-68/H cytotoxicity providing a useful model system to identify genes involved in the antiviral response and in the ultimate cell demise of virus-infected cells. Analysis of these gene expression changes identified several signaling pathways that may contribute to the susceptibility/resistance of tumor cells toward NDV. Considering previous NDV adsorption kinetic experiments [96] cells were infected for 12 hours at a multiplicity of infection according to the IC_{50} (13 virus particle/cell) value. Due to the infection 729 and 612 genes were up- or down-regulated, respectively, at least 2-fold. In the case of up-regulated genes more than 50 genes were induced 50-fold or higher and another 70 genes were expressed 10- to 50-fold of control cells. The prominent induction of

these genes is an expected effect of the strong antiviral response while the virus replicates and triggers apoptotic signaling.

Prior to these findings there had been only a limited number of transcriptome analyzes available in the literature investigating the gene expression alterations of cells after NDV infection [155, 156]. These publications analyzed up to 2950 cDNA elements and found about 50 genes maximal being altered upon NDV infection.

In order to try to classify the affected genes the DAVID functional annotation clustering tool was used [104]. The up- and down-regulated genes were classified into 176 and 146 overlapping clusters, respectively.

Several up-regulated gene clusters are involved in the innate immune response, inflammation and death signaling of the infected cells. Genes of cell cycle regulation and cellular metabolism were typically down-regulated.

7.7 MTH-68/H infection stimulates interferon-related pathways

A wide-range of tumor cells lack IFN expression and are thought to be highly selective to oncolytic viruses [91, 157, 158]. Meanwhile normal cells are capable to express different IFNs upon oncolytic virus infection, in tumor cells this protective mechanism is missing and are killed by other oncolytic activity of the virus. In wtPC12 cells as suggested by the microarray experiment the lack of IFN response cannot be responsible of the cytotoxicity of MTH-68/H in these cells. Although IFNα, IFNβ (Type I, viral), IFNγ (Type II, immune) and IFNλ (Type III) associated signaling pathways are strongly induced in wtPC12 cells with the subsequent induction of IFN stimulated genes (ISGs) upon NDV infection (Appendix 1, 2), this is not sufficient to prevent cells from apoptosis.

7.8 MTH-68/H infection induces cell cycle arrest

MTH-68/H infection of PC12 cells affected the expression of a number of cell cycle regulatory genes coding for both stimulators and inhibitors of cell cycle (Appendix 3-4). Genes were up- and down-regulated in both categories, but the overall balance of gene expression changes favours cell cycle arrest contributing to the anti-tumor effect of MTH-68/H.

7.9 Induction of apoptosis by MTH-68/H infection

A possible mechanism of cytotoxic activity of MTH-68/H in wtPC12 cells might be the induction of the different apoptotic pathways. Alterations at the level of mRNA were seen in the intrinsic, extrinsic apoptotic pathways as well as in the ER stress-related pathways in the gene expression pattern (Appendix 5-7).

As seen in Appendix 5 MTH-68/H only induces a few genes according to the intrinsic pathway of apoptosis (*Apaf1, Bid, Casp7*). This is not surprising as considered that the intrinsic pathway of apoptosis is highly regulated at the posttranslational level (e.g. phosphorylataion, dephosphorylation, oligomerization and proteolytic cleavage).

Furthermore the extrinsic pathway of apoptosis was induced in wtPC12 cells upon NDV infection (Appendix 6). Due to MTH-68/H infection wtPC12 cells express a high level of certain death ligands (*Tnf, Tnfsf10 [TRAIL], Faslg,* 35.4, 17.3, 2.2-fold increase, respectively) and related signaling molecules (e.g. *Ripk2, Ripk3, Birc2, Birc3, Fas. Tnf-r1*). Induction of the extrinsic pathway of apoptosis leads to subsequent proteolytic cleavage of caspase-8 and triggers the activation of effector caspase-7. Despite of the strong induction of *Tnf* gene, TNF evokes only a poor apoptotic response in PC12 cells (M. Pap and J. Szeberényi, unpublished results). Considering that FasL and its receptor were only poorly induced by MTH-68/H (*Faslg, Fas,* 2.2, 2.3-fold increase, respectively), TRAIL appears to be the most important autocrine/paracrine mediator of virus cytotoxicity parallel to the previous findings of Elankamuran et al., showing that TRAIL has a dominant role in the NDV-induced apoptosis [159] and might be proposed to be an important triggering molecule of MTH-68/H cytotoxicity.

NDV has been postulated to kill tumor cells according to several studies [85, 86, 160-165] by the stimulation of intrinsic and/or extrinsic pathways of programmed cell death [158, 166-169] or through ER stress-related apoptosis [85]. The data from the microarray experiments suggest that all three apoptotic pathways might be responsible for the MTH-68/H mediated oncolysis. As described by Fabian et al. MTH-68/H is able to replicate in wtPC12 cells and as a sign of evoked ER stress activation of caspase-12, phosphorylation of PERK and eIF2α was seen leading to cell death [85]. Virus particles utilize the secretion machinery of the host cell and induce UPR. A possible mechanism of the cytotoxic effect of MTH-68/H might be the overloading of the ER in wtPC12 cells. Overloading the ER leads to

the accumulation of misfolded/unfolded proteins, which in turn sequestrate BiP molecules and activate PERK, IRE1 and ATF6 pathways. As indicated by the microarray experiments MTH-68/H strongly induced several genes (*Casp4, Casp12, Ddit3, Atf3*) that code for proteins of the pro-apoptotic solution of ER stress (Appendix 7).

8 Summary

I. In the present thesis it was demonstrated that in addition to wtCREB overexpression, the expression of dominant mutant S129A, S133A and S129A-S133A CREB enhances the survival of PC12 cells.

II. In the signal transduction of ER stress GSK-3β and CREB seem to play a characteristic role. Pharmacological inhibition of GSK-3β enhanced survival in these cells and confirms GSK-3β to be a promising therapeutical target in ER stress related diseases.

III. CREB phosphorylation sites might regulate not only survival through altering the expression of Bcl-2 family members, but likely to promote changes in the cytoskeletal structure through the regulation of expression of microtubule-associated dynein-related proteins.

IV. In addition expression of any CREB construct used throughout the study might "steal" the CRE binding sites from ATF4 and ATF6 may temper the outcome of ER stress (Figure 22).

V. The present findings ascertain CREB as a potent inhibitor of the ER stress-signaling cascade. Identifying the possible mechanisms leading to increased viability might contribute to the understanding of the pathology of ER stress related disorders and could help to characterize ER stress related therapeutic targets.

VI. MTH-68/H induces a strong IFN response in wtPC12 cells, but this phenomenon alone cannot be responsible for the oncolysis of wtPC12 cells.

VII. MTH-68/H infection arrests cell cycle and pushes cells to cytostatic and cytocidal stage.

VIII. MTH-68/H induces the expression of genes being responsible for the intrinsic, extrinsic programmed cell death and ER stress related apoptosis.

9 References

1. Sela, M., F.H. White, Jr., and C.B. Anfinsen, *Reductive cleavage of disulfide bridges in ribonuclease.* Science, 1957. **125**(3250): p. 691-2.
2. Hetz, C., et al., *The unfolded protein response: integrating stress signals through the stress sensor IRE1alpha.* Physiol Rev, 2011. **91**(4): p. 1219-43.
3. Braakman, I. and N.J. Bulleid, *Protein folding and modification in the mammalian endoplasmic reticulum.* Annu Rev Biochem, 2011. **80**: p. 71-99.
4. Ellgaard, L. and A. Helenius, *Quality control in the endoplasmic reticulum.* Nat Rev Mol Cell Biol, 2003. **4**(3): p. 181-91.
5. Smith, M.H., H.L. Ploegh, and J.S. Weissman, *Road to ruin: targeting proteins for degradation in the endoplasmic reticulum.* Science, 2011. **334**(6059): p. 1086-90.
6. Glickman, M.H. and A. Ciechanover, *The ubiquitin-proteasome proteolytic pathway: destruction for the sake of construction.* Physiol Rev, 2002. **82**(2): p. 373-428.
7. Hammond, C., I. Braakman, and A. Helenius, *Role of N-linked oligosaccharide recognition, glucose trimming, and calnexin in glycoprotein folding and quality control.* Proc Natl Acad Sci U S A, 1994. **91**(3): p. 913-7.
8. Parodi, A.J., *Protein glucosylation and its role in protein folding.* Annu Rev Biochem, 2000. **69**: p. 69-93.
9. Walter, P. and D. Ron, *The unfolded protein response: from stress pathway to homeostatic regulation.* Science, 2011. **334**(6059): p. 1081-6.
10. Chakrabarti, A., A.W. Chen, and J.D. Varner, *A review of the mammalian unfolded protein response.* Biotechnol Bioeng, 2011. **108**(12): p. 2777-93.
11. Harding, H.P., Y. Zhang, and D. Ron, *Protein translation and folding are coupled by an endoplasmic-reticulum-resident kinase.* Nature, 1999. **397**(6716): p. 271-4.
12. Ameri, K. and A.L. Harris, *Activating transcription factor 4.* Int J Biochem Cell Biol, 2008. **40**(1): p. 14-21.
13. Harding, H.P., et al., *An integrated stress response regulates amino acid metabolism and resistance to oxidative stress.* Mol Cell, 2003. **11**(3): p. 619-33.
14. Lange, P.S., et al., *ATF4 is an oxidative stress-inducible, prodeath transcription factor in neurons in vitro and in vivo.* J Exp Med, 2008. **205**(5): p. 1227-42.
15. Hetz, C., *The unfolded protein response: controlling cell fate decisions under ER stress and beyond.* Nat Rev Mol Cell Biol, 2012. **13**(2): p. 89-102.
16. Scorrano, L., et al., *BAX and BAK regulation of endoplasmic reticulum Ca2+: a control point for apoptosis.* Science, 2003. **300**(5616): p. 135-9.
17. Wei, M.C., et al., *Proapoptotic BAX and BAK: a requisite gateway to mitochondrial dysfunction and death.* Science, 2001. **292**(5517): p. 727-30.
18. Zong, W.X., et al., *Bax and Bak can localize to the endoplasmic reticulum to initiate apoptosis.* J Cell Biol, 2003. **162**(1): p. 59-69.
19. Hetz, C., et al., *Proapoptotic BAX and BAK modulate the unfolded protein response by a direct interaction with IRE1alpha.* Science, 2006. **312**(5773): p. 572-6.
20. Danial, N.N. and S.J. Korsmeyer, *Cell death: critical control points.* Cell, 2004. **116**(2): p. 205-19.
21. Ow, Y.P., et al., *Cytochrome c: functions beyond respiration.* Nat Rev Mol Cell Biol, 2008. **9**(7): p. 532-42.
22. Hers, I., E.E. Vincent, and J.M. Tavare, *Akt signalling in health and disease.* Cell Signal, 2011. **23**(10): p. 1515-27.
23. Chen, W.S., et al., *Growth retardation and increased apoptosis in mice with homozygous disruption of the Akt1 gene.* Genes Dev, 2001. **15**(17): p. 2203-8.

24. Cho, H., et al., *Akt1/PKBalpha is required for normal growth but dispensable for maintenance of glucose homeostasis in mice.* J Biol Chem, 2001. **276**(42): p. 38349-52.
25. Cho, H., et al., *Insulin resistance and a diabetes mellitus-like syndrome in mice lacking the protein kinase Akt2 (PKB beta).* Science, 2001. **292**(5522): p. 1728-31.
26. Garofalo, R.S., et al., *Severe diabetes, age-dependent loss of adipose tissue, and mild growth deficiency in mice lacking Akt2/PKB beta.* J Clin Invest, 2003. **112**(2): p. 197-208.
27. Vanhaesebroeck, B., et al., *The emerging mechanisms of isoform-specific PI3K signalling.* Nat Rev Mol Cell Biol, 2010. **11**(5): p. 329-41.
28. Forde, J.E. and T.C. Dale, *Glycogen synthase kinase 3: a key regulator of cellular fate.* Cell Mol Life Sci, 2007. **64**(15): p. 1930-44.
29. Jope, R.S. and G.V. Johnson, *The glamour and gloom of glycogen synthase kinase-3.* Trends Biochem Sci, 2004. **29**(2): p. 95-102.
30. Pap, M. and G.M. Cooper, *Role of translation initiation factor 2B in control of cell survival by the phosphatidylinositol 3-kinase/Akt/glycogen synthase kinase 3beta signaling pathway.* Mol Cell Biol, 2002. **22**(2): p. 578-86.
31. Boyle, W.J., et al., *Activation of protein kinase C decreases phosphorylation of c-Jun at sites that negatively regulate its DNA-binding activity.* Cell, 1991. **64**(3): p. 573-84.
32. Beals, C.R., et al., *Nuclear export of NF-ATc enhanced by glycogen synthase kinase-3.* Science, 1997. **275**(5308): p. 1930-4.
33. Neal, J.W. and N.A. Clipstone, *Glycogen synthase kinase-3 inhibits the DNA binding activity of NFATc.* J Biol Chem, 2001. **276**(5): p. 3666-73.
34. Chu, B., et al., *Sequential phosphorylation by mitogen-activated protein kinase and glycogen synthase kinase 3 represses transcriptional activation by heat shock factor-1.* J Biol Chem, 1996. **271**(48): p. 30847-57.
35. Grimes, C.A. and R.S. Jope, *CREB DNA binding activity is inhibited by glycogen synthase kinase-3 beta and facilitated by lithium.* J Neurochem, 2001. **78**(6): p. 1219-32.
36. Tullai, J.W., et al., *Glycogen synthase kinase-3 represses cyclic AMP response element-binding protein (CREB)-targeted immediate early genes in quiescent cells.* J Biol Chem, 2007. **282**(13): p. 9482-91.
37. Doble, B.W. and J.R. Woodgett, *GSK-3: tricks of the trade for a multi-tasking kinase.* J Cell Sci, 2003. **116**(Pt 7): p. 1175-86.
38. Beurel, E. and R.S. Jope, *The paradoxical pro- and anti-apoptotic actions of GSK3 in the intrinsic and extrinsic apoptosis signaling pathways.* Prog Neurobiol, 2006. **79**(4): p. 173-89.
39. Pap, M. and G.M. Cooper, *Role of glycogen synthase kinase-3 in the phosphatidylinositol 3-Kinase/Akt cell survival pathway.* J Biol Chem, 1998. **273**(32): p. 19929-32.
40. Watcharasit, P., et al., *Direct, activating interaction between glycogen synthase kinase-3beta and p53 after DNA damage.* Proc Natl Acad Sci U S A, 2002. **99**(12): p. 7951-5.
41. Loberg, R.D., E. Vesely, and F.C. Brosius, 3rd, *Enhanced glycogen synthase kinase-3beta activity mediates hypoxia-induced apoptosis of vascular smooth muscle cells and is prevented by glucose transport and metabolism.* J Biol Chem, 2002. **277**(44): p. 41667-73.
42. Song, L., P. De Sarno, and R.S. Jope, *Central role of glycogen synthase kinase-3beta in endoplasmic reticulum stress-induced caspase-3 activation.* J Biol Chem, 2002. **277**(47): p. 44701-8.
43. Kotla, S., et al., *The transcription factor CREB enhances interleukin-17A production and inflammation in a mouse model of atherosclerosis.* Sci Signal, 2013. **6**(293): p. ra83.
44. Schauer, I.E., et al., *CREB downregulation in vascular disease: a common response to cardiovascular risk.* Arterioscler Thromb Vasc Biol, 2010. **30**(4): p. 733-41.

45. Mayr, B. and M. Montminy, *Transcriptional regulation by the phosphorylation-dependent factor CREB.* Nat Rev Mol Cell Biol, 2001. **2**(8): p. 599-609.
46. Fiol, C.J., et al., *A secondary phosphorylation of CREB341 at Ser129 is required for the cAMP-mediated control of gene expression. A role for glycogen synthase kinase-3 in the control of gene expression.* J Biol Chem, 1994. **269**(51): p. 32187-93.
47. Bullock, B.P. and J.F. Habener, *Phosphorylation of the cAMP response element binding protein CREB by cAMP-dependent protein kinase A and glycogen synthase kinase-3 alters DNA-binding affinity, conformation, and increases net charge.* Biochemistry, 1998. **37**(11): p. 3795-809.
48. Lee, A.S., *The glucose-regulated proteins: stress induction and clinical applications.* Trends Biochem Sci, 2001. **26**(8): p. 504-10.
49. Lee, A.S., *Mammalian stress response: induction of the glucose-regulated protein family.* Curr Opin Cell Biol, 1992. **4**(2): p. 267-73.
50. Balasubramanyam, M., R. Lenin, and F. Monickaraj, *Endoplasmic reticulum stress in diabetes: New insights of clinical relevance.* Indian J Clin Biochem, 2010. **25**(2): p. 111-8.
51. Wang, S. and R.J. Kaufman, *The impact of the unfolded protein response on human disease.* J Cell Biol, 2012. **197**(7): p. 857-67.
52. Verfaillie, T., A.D. Garg, and P. Agostinis, *Targeting ER stress induced apoptosis and inflammation in cancer.* Cancer Lett, 2010.
53. Mekahli, D., et al., *Endoplasmic-reticulum calcium depletion and disease.* Cold Spring Harb Perspect Biol, 2011. **3**(6).
54. Li, W.W., et al., *Transactivation of the grp78 promoter by Ca2+ depletion. A comparative analysis with A23187 and the endoplasmic reticulum Ca(2+)-ATPase inhibitor thapsigargin.* J Biol Chem, 1993. **268**(16): p. 12003-9.
55. Treiman, M., C. Caspersen, and S.B. Christensen, *A tool coming of age: thapsigargin as an inhibitor of sarco-endoplasmic reticulum Ca(2+)-ATPases.* Trends Pharmacol Sci, 1998. **19**(4): p. 131-5.
56. Heifetz, A., R.W. Keenan, and A.D. Elbein, *Mechanism of action of tunicamycin on the UDP-GlcNAc:dolichyl-phosphate Glc-NAc-1-phosphate transferase.* Biochemistry, 1979. **18**(11): p. 2186-92.
57. Breitling, J. and M. Aebi, *N-linked protein glycosylation in the endoplasmic reticulum.* Cold Spring Harb Perspect Biol, 2013. **5**(8): p. a013359.
58. Ji, C., *Mechanisms of alcohol-induced endoplasmic reticulum stress and organ injuries.* Biochem Res Int, 2012. **2012**: p. 216450.
59. Ramirez, T., et al., *Chronic alcohol-induced hepatic insulin resistance and endoplasmic reticulum stress ameliorated by peroxisome-proliferator activated receptor-delta agonist treatment.* J Gastroenterol Hepatol, 2013. **28**(1): p. 179-87.
60. Kaphalia, L., et al., *Ethanol metabolism, oxidative stress, and endoplasmic reticulum stress responses in the lungs of hepatic alcohol dehydrogenase deficient deer mice after chronic ethanol feeding.* Toxicol Appl Pharmacol, 2014. **277**(2): p. 109-117.
61. He, B., *Viruses, endoplasmic reticulum stress, and interferon responses.* Cell Death Differ, 2006. **13**(3): p. 393-403.
62. Lin, J.H., P. Walter, and T.S. Yen, *Endoplasmic reticulum stress in disease pathogenesis.* Annu Rev Pathol, 2008. **3**: p. 399-425.
63. Samuel, C.E., *Antiviral actions of interferons.* Clin Microbiol Rev, 2001. **14**(4): p. 778-809, table of contents.
64. Sadler, A.J. and B.R. Williams, *Interferon-inducible antiviral effectors.* Nat Rev Immunol, 2008. **8**(7): p. 559-68.

65. Pap, M. and J. Szeberenyi, *Involvement of proteolytic activation of protein kinase R in the apoptosis of PC12 pheochromocytoma cells.* Cell Mol Neurobiol, 2008. **28**(3): p. 443-56.
66. Chou, J. and B. Roizman, *Herpes simplex virus 1 gamma(1)34.5 gene function, which blocks the host response to infection, maps in the homologous domain of the genes expressed during growth arrest and DNA damage.* Proc Natl Acad Sci U S A, 1994. **91**(12): p. 5247-51.
67. Whitley, R.J., et al., *Replication, establishment of latency, and induced reactivation of herpes simplex virus gamma 1 34.5 deletion mutants in rodent models.* J Clin Invest, 1993. **91**(6): p. 2837-43.
68. Boyce, M., et al., *A selective inhibitor of eIF2alpha dephosphorylation protects cells from ER stress.* Science, 2005. **307**(5711): p. 935-9.
69. Zhang, L. and A. Wang, *Virus-induced ER stress and the unfolded protein response.* Front Plant Sci, 2012. **3**: p. 293.
70. Bitko, V. and S. Barik, *An endoplasmic reticulum-specific stress-activated caspase (caspase-12) is implicated in the apoptosis of A549 epithelial cells by respiratory syncytial virus.* J Cell Biochem, 2001. **80**(3): p. 441-54.
71. Peluso, R.W., R.A. Lamb, and P.W. Choppin, *Infection with paramyxoviruses stimulates synthesis of cellular polypeptides that are also stimulated in cells transformed by Rous sarcoma virus or deprived of glucose.* Proc Natl Acad Sci U S A, 1978. **75**(12): p. 6120-4.
72. Peluso, R.W., R.A. Lamb, and P.W. Choppin, *Polypeptide synthesis in simian virus 5-infected cells.* J Virol, 1977. **23**(1): p. 177-87.
73. Jordan, R., et al., *Replication of a cytopathic strain of bovine viral diarrhea virus activates PERK and induces endoplasmic reticulum stress-mediated apoptosis of MDBK cells.* J Virol, 2002. **76**(19): p. 9588-99.
74. Su, H.L., C.L. Liao, and Y.L. Lin, *Japanese encephalitis virus infection initiates endoplasmic reticulum stress and an unfolded protein response.* J Virol, 2002. **76**(9): p. 4162-71.
75. Li, X.D., et al., *Tula hantavirus triggers pro-apoptotic signals of ER stress in Vero E6 cells.* Virology, 2005. **333**(1): p. 180-9.
76. Bartlett, D.L., et al., *Oncolytic viruses as therapeutic cancer vaccines.* Mol Cancer, 2013. **12**(1): p. 103.
77. Chiocca, E.A., *Oncolytic viruses.* Nat Rev Cancer, 2002. **2**(12): p. 938-50.
78. Parato, K.A., et al., *Recent progress in the battle between oncolytic viruses and tumours.* Nat Rev Cancer, 2005. **5**(12): p. 965-76.
79. Varghese, S. and S.D. Rabkin, *Oncolytic herpes simplex virus vectors for cancer virotherapy.* Cancer Gene Ther, 2002. **9**(12): p. 967-78.
80. Zeyaullah, M., et al., *Oncolytic viruses in the treatment of cancer: a review of current strategies.* Pathol Oncol Res, 2012. **18**(4): p. 771-81.
81. Vacchelli, E., et al., *Trial watch: Oncolytic viruses for cancer therapy.* Oncoimmunology, 2013. **2**(6): p. e24612.
82. Donahue, J.M., J.T. Mullen, and K.K. Tanabe, *Viral oncolysis.* Surg Oncol Clin N Am, 2002. **11**(3): p. 661-80.
83. Alexander, D.J., *Newcastle disease and other avian paramyxoviruses.* Rev Sci Tech, 2000. **19**(2): p. 443-62.
84. Csatary, L.K., et al., *Attenuated veterinary virus vaccine for the treatment of cancer.* Cancer Detect Prev, 1993. **17**(6): p. 619-27.
85. Fabian, Z., et al., *p53-independent endoplasmic reticulum stress-mediated cytotoxicity of a Newcastle disease virus strain in tumor cell lines.* J Virol, 2007. **81**(6): p. 2817-30.
86. Szeberenyi, J., et al., *Newcastle disease virus-induced apoptosis in PC12 pheochromocytoma cells.* Am J Ther, 2003. **10**(4): p. 282-8.

87. Csatary, L.K., et al., *MTH-68/H oncolytic viral treatment in human high-grade gliomas.* J Neurooncol, 2004. **67**(1-2): p. 83-93.
88. Eager, R.M. and J. Nemunaitis, *Clinical development directions in oncolytic viral therapy.* Cancer Gene Ther, 2011. **18**(5): p. 305-17.
89. Liu, T.C., E. Galanis, and D. Kirn, *Clinical trial results with oncolytic virotherapy: a century of promise, a decade of progress.* Nat Clin Pract Oncol, 2007. **4**(2): p. 101-17.
90. Lorence, R.M., et al., *Overview of phase I studies of intravenous administration of PV701, an oncolytic virus.* Curr Opin Mol Ther, 2003. **5**(6): p. 618-24.
91. Lorence, R.M., et al., *Phase 1 clinical experience using intravenous administration of PV701, an oncolytic Newcastle disease virus.* Curr Cancer Drug Targets, 2007. **7**(2): p. 157-67.
92. Pecora, A.L., et al., *Phase I trial of intravenous administration of PV701, an oncolytic virus, in patients with advanced solid cancers.* J Clin Oncol, 2002. **20**(9): p. 2251-66.
93. Vaha-Koskela, M.J., J.E. Heikkila, and A.E. Hinkkanen, *Oncolytic viruses in cancer therapy.* Cancer Lett, 2007. **254**(2): p. 178-216.
94. Csatary, L.K. and T. Bakacs, *Use of Newcastle disease virus vaccine (MTH-68/H) in a patient with high-grade glioblastoma.* Jama, 1999. **281**(17): p. 1588-9.
95. Freeman, A.I., et al., *Phase I/II trial of intravenous NDV-HUJ oncolytic virus in recurrent glioblastoma multiforme.* Mol Ther, 2006. **13**(1): p. 221-8.
96. Balogh, A., et al., *A simple fluorescent labeling technique to study virus adsorption in Newcastle disease virus infected cells.* Enzyme Microb Technol, 2011. **49**(3): p. 255-9.
97. Copeland, N.G. and G.M. Cooper, *Transfection by exogenous and endogenous murine retrovirus DNAs.* Cell, 1979. **16**(2): p. 347-56.
98. Jope, R.S., *Lithium and GSK-3: one inhibitor, two inhibitory actions, multiple outcomes.* Trends Pharmacol Sci, 2003. **24**(9): p. 441-3.
99. Puthalakath, H., et al., *ER stress triggers apoptosis by activating BH3-only protein Bim.* Cell, 2007. **129**(7): p. 1337-49.
100. Reed, J.C., *Proapoptotic multidomain Bcl-2/Bax-family proteins: mechanisms, physiological roles, and therapeutic opportunities.* Cell Death Differ, 2006. **13**(8): p. 1378-86.
101. Hübner, A., et al., *Multisite phosphorylation regulates Bim stability and apoptotic activity.* Mol Cell, 2008. **30**(4): p. 415-25.
102. Echeverry, N., et al., *Intracellular localization of the BCL-2 family member BOK and functional implications.* Cell Death Differ, 2013. **20**(6): p. 785-99.
103. Puthalakath, H., et al., *The proapoptotic activity of the Bcl-2 family member Bim is regulated by interaction with the dynein motor complex.* Mol Cell, 1999. **3**(3): p. 287-96.
104. Huang da, W., B.T. Sherman, and R.A. Lempicki, *Systematic and integrative analysis of large gene lists using DAVID bioinformatics resources.* Nat Protoc, 2009. **4**(1): p. 44-57.
105. Grimes, C.A. and R.S. Jope, *The multifaceted roles of glycogen synthase kinase 3beta in cellular signaling.* Prog Neurobiol, 2001. **65**(4): p. 391-426.
106. Rudolph, D., et al., *Impaired fetal T cell development and perinatal lethality in mice lacking the cAMP response element binding protein.* Proc Natl Acad Sci U S A, 1998. **95**(8): p. 4481-6.
107. Jean, D., et al., *CREB and its associated proteins act as survival factors for human melanoma cells.* J Biol Chem, 1998. **273**(38): p. 24884-90.
108. Bonni, A., et al., *Cell survival promoted by the Ras-MAPK signaling pathway by transcription-dependent and -independent mechanisms.* Science, 1999. **286**(5443): p. 1358-62.
109. Walton, M., et al., *CREB phosphorylation promotes nerve cell survival.* J Neurochem, 1999. **73**(5): p. 1836-42.

110. Greene, L.A. and A.S. Tischler, *Establishment of a noradrenergic clonal line of rat adrenal pheochromocytoma cells which respond to nerve growth factor.* Proc Natl Acad Sci U S A, 1976. **73**(7): p. 2424-8.
111. Hiroi, T., et al., *Protracted lithium treatment protects against the ER stress elicited by thapsigargin in rat PC12 cells: roles of intracellular calcium, GRP78 and Bcl-2.* Pharmacogenomics J, 2005. **5**(2): p. 102-11.
112. Takadera, T., R. Yoshikawa, and T. Ohyashiki, *Thapsigargin-induced apoptosis was prevented by glycogen synthase kinase-3 inhibitors in PC12 cells.* Neurosci Lett, 2006. **408**(2): p. 124-8.
113. Takadera, T., et al., *Caspase-dependent apoptosis induced by thapsigargin was prevented by glycogen synthase kinase-3 inhibitors in cultured rat cortical neurons.* Neurochem Res, 2007. **32**(8): p. 1336-42.
114. Faundez, V., J.T. Horng, and R.B. Kelly, *ADP ribosylation factor 1 is required for synaptic vesicle budding in PC12 cells.* J Cell Biol, 1997. **138**(3): p. 505-15.
115. Cleves, A.E., L. Clift-O'Grady, and R.B. Kelly, *ATP-dependent formation of free synaptic vesicles from PC12 membranes in vitro.* Neurochem Res, 1997. **22**(8): p. 933-40.
116. Rosa, P., et al., *Brefeldin A inhibits the formation of constitutive secretory vesicles and immature secretory granules from the trans-Golgi network.* Eur J Cell Biol, 1992. **59**(2): p. 265-74.
117. Chen, L. and X. Gao, *Neuronal apoptosis induced by endoplasmic reticulum stress.* Neurochem Res, 2002. **27**(9): p. 891-8.
118. Elyaman, W., C. Yardin, and J. Hugon, *Involvement of glycogen synthase kinase-3beta and tau phosphorylation in neuronal Golgi disassembly.* J Neurochem, 2002. **81**(4): p. 870-80.
119. Kogel, D., et al., *The amyloid precursor protein protects PC12 cells against endoplasmic reticulum stress-induced apoptosis.* J Neurochem, 2003. **87**(1): p. 248-56.
120. Sasaya, H., et al., *Nicotine suppresses tunicamycin-induced, but not thapsigargin-induced, expression of GRP78 during ER stress-mediated apoptosis in PC12 cells.* J Biochem, 2008. **144**(2): p. 251-7.
121. Utsumi, T., et al., *Protective effect of nicotine on tunicamycin-induced apoptosis of PC12h cells.* Neurosci Lett, 2004. **370**(2-3): p. 244-7.
122. Gonzalez, G.A. and M.R. Montminy, *Cyclic AMP stimulates somatostatin gene transcription by phosphorylation of CREB at serine 133.* Cell, 1989. **59**(4): p. 675-80.
123. Wang, Q.M., P.J. Roach, and C.J. Fiol, *Use of a synthetic peptide as a selective substrate for glycogen synthase kinase 3.* Anal Biochem, 1994. **220**(2): p. 397-402.
124. Ozaki, N. and D.M. Chuang, *Lithium increases transcription factor binding to AP-1 and cyclic AMP-responsive element in cultured neurons and rat brain.* J Neurochem, 1997. **69**(6): p. 2336-44.
125. Tullai, J.W., J.R. Graham, and G.M. Cooper, *A GSK-3-mediated transcriptional network maintains repression of immediate early genes in quiescent cells.* Cell Cycle, 2011. **10**(18): p. 3072-7.
126. Zhang, X., et al., *Genome-wide analysis of cAMP-response element binding protein occupancy, phosphorylation, and target gene activation in human tissues.* Proc Natl Acad Sci U S A, 2005. **102**(12): p. 4459-64.
127. Impey, S., et al., *Defining the CREB regulon: a genome-wide analysis of transcription factor regulatory regions.* Cell, 2004. **119**(7): p. 1041-54.
128. Conkright, M.D., et al., *Genome-wide analysis of CREB target genes reveals a core promoter requirement for cAMP responsiveness.* Mol Cell, 2003. **11**(4): p. 1101-8.
129. Lemaigre, F.P., C.I. Ace, and M.R. Green, *The cAMP response element binding protein, CREB, is a potent inhibitor of diverse transcriptional activators.* Nucleic Acids Res, 1993. **21**(12): p. 2907-11.

130. Seo, H.Y., et al., *Endoplasmic reticulum stress-induced activation of activating transcription factor 6 decreases cAMP-stimulated hepatic gluconeogenesis via inhibition of CREB.* Endocrinology, 2010. **151**(2): p. 561-8.
131. Wang, Y., et al., *The CREB coactivator CRTC2 links hepatic ER stress and fasting gluconeogenesis.* Nature, 2009. **460**(7254): p. 534-7.
132. Wilson, B.E., E. Mochon, and L.M. Boxer, *Induction of bcl-2 expression by phosphorylated CREB proteins during B-cell activation and rescue from apoptosis.* Mol Cell Biol, 1996. **16**(10): p. 5546-56.
133. Freeland, K., L.M. Boxer, and D.S. Latchman, *The cyclic AMP response element in the Bcl-2 promoter confers inducibility by hypoxia in neuronal cells.* Brain Res Mol Brain Res, 2001. **92**(1-2): p. 98-106.
134. Pugazhenthi, S., et al., *Akt/protein kinase B up-regulates Bcl-2 expression through cAMP-response element-binding protein.* J Biol Chem, 2000. **275**(15): p. 10761-6.
135. Wang, W. and M. Zheng, *Role of cAMP-PKA/CREB pathway in regulation of AQP 5 production in rat nasal epithelium.* Rhinology, 2011. **49**(4): p. 464-9.
136. Wang, L., et al., *PDGF-induced proliferation of smooth muscular cells is related to the regulation of CREB phosphorylation and Nur77 expression.* J Huazhong Univ Sci Technolog Med Sci, 2011. **31**(2): p. 169-73.
137. Wang, A. and J.A. Bibb, *Is CREB the angry bird that releases memory in Alzheimer's?* Neuropsychopharmacology, 2011. **36**(11): p. 2153-4.
138. Gao, H.L., et al., *Disruption of the CaMKII/CREB signaling is associated with zinc deficiency-induced learning and memory impairments.* Neurotox Res, 2011. **19**(4): p. 584-91.
139. Harada, H., et al., *Survival factor-induced extracellular signal-regulated kinase phosphorylates BIM, inhibiting its association with BAX and proapoptotic activity.* Proc Natl Acad Sci U S A, 2004. **101**(43): p. 15313-7.
140. Gao, X., et al., *Identification of nucleolar and coiled-body phosphoprotein 1 (NOLC1) minimal promoter regulated by NF-kappaB and CREB.* BMB Rep, 2011. **44**(1): p. 70-5.
141. Li, X.Y., et al., *CREB is a regulatory target for the protein kinase Akt/PKB in the differentiation of pancreatic ductal cells into islet beta-cells mediated by hepatocyte growth factor.* Biochem Biophys Res Commun, 2011. **404**(2): p. 711-6.
142. O'Connor, L., et al., *Bim: a novel member of the Bcl-2 family that promotes apoptosis.* EMBO J, 1998. **17**(2): p. 384-95.
143. Biswas, S.C. and L.A. Greene, *Nerve growth factor (NGF) down-regulates the Bcl-2 homology 3 (BH3) domain-only protein Bim and suppresses its proapoptotic activity by phosphorylation.* J Biol Chem, 2002. **277**(51): p. 49511-6.
144. Ley, R., et al., *Extracellular signal-regulated kinases 1/2 are serum-stimulated "Bim(EL) kinases" that bind to the BH3-only protein Bim(EL) causing its phosphorylation and turnover.* J Biol Chem, 2004. **279**(10): p. 8837-47.
145. Luciano, F., et al., *Phosphorylation of Bim-EL by Erk1/2 on serine 69 promotes its degradation via the proteasome pathway and regulates its proapoptotic function.* Oncogene, 2003. **22**(43): p. 6785-93.
146. Marani, M., et al., *Role of Bim in the survival pathway induced by Raf in epithelial cells.* Oncogene, 2004. **23**(14): p. 2431-41.
147. Lei, K. and R.J. Davis, *JNK phosphorylation of Bim-related members of the Bcl2 family induces Bax-dependent apoptosis.* Proc Natl Acad Sci U S A, 2003. **100**(5): p. 2432-7.
148. Weston, C.R., et al., *Activation of ERK1/2 by deltaRaf-1:ER* represses Bim expression independently of the JNK or PI3K pathways.* Oncogene, 2003. **22**(9): p. 1281-93.

149. Funakoshi, Y., et al., *Critical role of cAMP-response element-binding protein for angiotensin II-induced hypertrophy of vascular smooth muscle cells.* J Biol Chem, 2002. **277**(21): p. 18710-7.
150. Hall, J.L., et al., *Upregulation of glucose metabolism during intimal lesion formation is coupled to the inhibition of vascular smooth muscle cell apoptosis. Role of GSK3beta.* Diabetes, 2001. **50**(5): p. 1171-9.
151. Reusch, J.E. and P.A. Watson, *Loss of CREB regulation of vascular smooth muscle cell quiescence in diabetes.* Rev Endocr Metab Disord, 2004. **5**(3): p. 209-19.
152. Tokunou, T., et al., *Apoptosis induced by inhibition of cyclic AMP response element-binding protein in vascular smooth muscle cells.* Circulation, 2003. **108**(10): p. 1246-52.
153. Zhang, J., et al., *Cyclic AMP inhibits p38 activation via CREB-induced dynein light chain.* Mol Cell Biol, 2006. **26**(4): p. 1223-34.
154. Zhang, J., et al., *Cyclic AMP inhibits JNK activation by CREB-mediated induction of c-FLIP(L) and MKP-1, thereby antagonizing UV-induced apoptosis.* Cell Death Differ, 2008. **15**(10): p. 1654-62.
155. Munir, S., J.M. Sharma, and V. Kapur, *Transcriptional response of avian cells to infection with Newcastle disease virus.* Virus Res, 2005. **107**(1): p. 103-8.
156. Krishnamurthy, S., et al., *Differentially regulated interferon response determines the outcome of Newcastle disease virus infection in normal and tumor cell lines.* J Virol, 2006. **80**(11): p. 5145-55.
157. Stojdl, D.F., et al., *Exploiting tumor-specific defects in the interferon pathway with a previously unknown oncolytic virus.* Nat Med, 2000. **6**(7): p. 821-5.
158. Elankumaran, S., et al., *Type I interferon-sensitive recombinant newcastle disease virus for oncolytic virotherapy.* J Virol, 2010. **84**(8): p. 3835-44.
159. Elankumaran, S., D. Rockemann, and S.K. Samal, *Newcastle disease virus exerts oncolysis by both intrinsic and extrinsic caspase-dependent pathways of cell death.* J Virol, 2006. **80**(15): p. 7522-34.
160. Fabian, Z., et al., *Induction of apoptosis by a Newcastle disease virus vaccine (MTH-68/H) in PC12 rat phaeochromocytoma cells.* Anticancer Res, 2001. **21**(1A): p. 125-35.
161. Zulkifli, M.M., et al., *Newcastle diseases virus strain V4UPM displayed oncolytic ability against experimental human malignant glioma.* Neurol Res, 2009. **31**(1): p. 3-10.
162. Alabsi, A.M., et al., *Anti-leukemic activity of Newcastle disease virus strains AF2240 and V4-UPM in murine myelomonocytic leukemia in vivo.* Leuk Res, 2012. **36**(5): p. 634-45.
163. Alabsi, A.M., et al., *Effects of newcastle disease virus strains AF2240 and V4-UPM on cytolysis and apoptosis of leukemia cell lines.* Int J Mol Sci, 2011. **12**(12): p. 8645-60.
164. Ali, R., et al., *Cytolytic effects and apoptosis induction of Newcastle disease virus strain AF2240 on anaplastic astrocytoma brain tumor cell line.* Neurochem Res, 2011. **36**(11): p. 2051-62.
165. Wu, Y., et al., *Apoptin enhances the oncolytic properties of Newcastle disease virus.* Intervirology, 2012. **55**(4): p. 276-86.
166. Fu, F., et al., *Antiproliferative effect of newcastle disease virus strain D90 on human lung cancer cell line A549.* Oncol Res, 2011. **19**(7): p. 323-33.
167. Meng, S., et al., *Newcastle disease virus induces apoptosis in cisplatin-resistant human lung adenocarcinoma A549 cells in vitro and in vivo.* Cancer Lett, 2012. **317**(1): p. 56-64.
168. Molouki, A., et al., *Newcastle disease virus infection promotes Bax redistribution to mitochondria and cell death in HeLa cells.* Intervirology, 2010. **53**(2): p. 87-94.
169. Yaacov, B., et al., *Selective oncolytic effect of an attenuated Newcastle disease virus (NDV-HUJ) in lung tumors.* Cancer Gene Ther, 2008. **15**(12): p. 795-807.

10 Appendix

Appendix 1 The effect of MTH-68/H infection on the expression of genes involved in the induction of type I IFN genes in PC12 cells

Gene/Protein		Protein function	Induction/repression by MTH-68/H (fold) [a,b]
Genes of RIG-I-like receptor pathways			
10869879	similar to IFNα 8/6 precursor	cytokine (putative)	80.3↑
Ddx60	DEAD box polypeptide 60	cytosolic viral RNA receptor/helicase	67.3↑
Ifnb1	IFN β1	cytokine/type I IFN	49.5↑
Ifih1 (MDA5)	IFN-induced with helicase C domain 1 (melanoma differentiation-associated gene 5)	cytosolic viral RNA receptor/helicase	36.6↑
Irf7	IFN regulatory factor 7	transcription factor	23.5↑
Ddx58 (RIG-I)	DEAD box polypeptide 58 (retinoic acid inducible gene-I)	cytosolic viral RNA receptor/helicase	18.8↑
Ifnb2 (IL6)	IFN β2 (interleukin 6)	cytokine	15.2↑
Dhx58 (LGP2)	DEXH box polypeptide 58 (laboratory of genetics and physiology 2)	cytosolic viral RNA receptor/helicase	10.7↑
Trim25	tripartite motif-containing 25	E3 ubiquitin/ISG15 ligase	6.2↑
Ifna11	IFN α11	cytokine/type I IFN	4.0↑
Ifna4	IFN α4	cytokine/type I IFN	3.6↑
Ifna1	IFN α1	cytokine/type I IFN	3.4↑
Mavs (IPS-1)	mitochondrial antiviral signal adapter (IFNβ stimulator protein-1)	adapter protein	NSA[c]
Traf3	TNF receptor-associated factor 3	E3 ubiquitin ligase/adapter protein	NSA
ATank	TRAF-associated NFκB activator	adapter protein	NSA

Appendix 1 continued

Ikbke	IκB kinase ε	serine-threonine kinase	NSA
Irf3	IFN regulatory factor 3	transcription factor	NSA
Tbk1	TANK-binding kinase 1	serine-threonine kinase	NSA
Traf6	TNF receptor-associated factor 6	E3 ubiquitin ligase/adapter protein	NSA
Genes of Toll-like receptor pathways			
Nfkbie	NFκB inhibitor ε	IκB ε	8.1↑
Nfkbiz	NFκB inhibitor z	IκB z	6.0↑
Tlr3	toll-like receptor 3	transmembrane receptor	4.1↑
Nfkbid	NFκB inhibitor δ	IκB δ	3.6↑
Nfkbia	NFκB inhibitor α	IκBα	3.3↑
Nfkb2	nuclear factor κB2 (NFκB2)	transcription factor	3.0↑
Nfkb1	nuclear factor κB1 (NFκB1)	transcription factor	2.8↑
MyD88	myeloid differentiation early response gene 88	adapter protein	2.1↑
Nfkbib	NFκB inhibitor β	IκB β	2.0↑
Ikbkb (IKKβ)	IκB kinase β	serine-threonine kinase	NSA
Ikbkg (NEMO)	IκB kinase γ (NFκB essential modulator)	adapter protein	NSA
Traf6	TNF receptor-associated factor 6	E3 ubiquitin ligase/adapter protein	NSA
Irak1	IL-1 receptor-activated kinase 1	serine-threonine kinase	NSA

Appendix 1 continued

Irak4	IL-1 receptor-activated kinase 4	serine-threonine kinase	NSA
Ripk1	receptor-interacting serine-threonine	serine-threonine kinase	NSA
kinase 1			
Traf3	TNF receptor-associated factor 3	E3 ubiquitin ligase/adapter protein	NSA
Trif	TIR-domain containing adapter inducing IFNβ	adapter protein	NSA
Tak1	TGFβ-activated kinase 1	serine-threonine kinase	NSA
Ikbka	IκB kinase α	serine-threonine kinase	NSA
Tlr7/8	toll-like receptor 7/8	transmembrane receptor	ND[d]
Tlr9	toll-like receptor 9	transmembrane receptor	ND
Tab1	TAK1 binding protein 1	adapter protein	ND
Tab3	TAK1 binding protein 3	adapter protein	ND

[a] PC12 cells were infected with MTH-68/H at IC_{50} for 12 hours. Steady-state levels of mRNAs were determined using oligonucleotide microarrays as described in Materials and Methods.

[b] Induction and repression of genes are indicated by upward and downward arrows, respectively.

[c] Gene expression was not significantly altered (less than 2-fold induction or repression) by MTH-68/H.

[d] Gene expression was not detected by the microarray.

Appendix 2 Expression of genes involved in IFN-signaling in MTH-68/H-infected PC12 cells

Gene/Protein		Protein function	Induction/repression by MTH-68/H (fold) [1,2]
Signaling to ISRE and GAS enhancer elements			
10869879	similar to IFNα 8/6 precursor	cytokine (putative)	80.3↑
Ifnb1	IFN β1	cytokine/type I IFN	49.5↑
10720237	similar to IFN λ2	cytokine/type III IFN (putative)	23.0↑
Ifnb2 (IL6)	IFN β2 (interleukin 6)	cytokine	15.2↑
Stat2	signal transducer and activator of transcription 2	transcription factor	12.4↑
Stat1	signal transducer and activator of transcription 1	transcription factor	7.3↑
Irf9	interferon regulatory factor 9	transcription factor	6.2↑
Ifna11	IFN α11	cytokine/type I IFN	4.0↑
Ifna4	IFN α4	cytokine/type I IFN	3.6↑
Jak2	Janus kinase 2	non-receptor tyrosine protein kinase	3.4↑
Ifna1	IFN α1	cytokine/type I IFN	3.4↑
Ifngr1	IFN γ receptor 1	type II IFN receptor	NSA[3]
Ifngr2	IFN γ receptor 2	type II IFN receptor	NSA
Ifnlr1	IFN λ receptor 1	type III IFN receptor	NSA
Il10r2	IL10 receptor 2	type III IFN receptor/IL10 receptor	NSA
Ifnar1	IFN α receptor 1	type I IFN receptor	NSA
Jak1	Janus kinase 1	non-receptor tyrosine protein kinase	NSA
Tyk2	tyrosine kinase 2	non-receptor tyrosine protein kinase	ND[4]
Ifng	IFN γ	cytokine/type II IFN	ND
Ifnar2	IFN α receptor 2	type I IFN receptor	ND

Appendix 2 continued

Type I IFN effector pathways			
ISGylation pathways			
Isg15	IFN-stimulated gene 15	ubiquitin-like protein	30.4↑
Herc6	HECT domain and RLD containing protein 6	E3 ubiquitin/ISG15 ligase	28.7↑
Usp18	ubiquitin-specific peptidase 18	de-ISGylating protease	27.8↑
Uba7	ubiquitin-activating enzyme 7	E1 ubiquitin/ISG15 activating enzyme	13.2↑
Trim25	tripartite motif-containing protein 25	E3 ubiquitin/ISG15 ligase	6.2↑
Usp49	ubiquitin-specific peptidase 49	de-ISGylating protease	3.1↑
Ube2E1	ubiquitin-conjugating enzyme E1	E2 ubiquitin/ISG15 conjugating enzyme	2.4↑
Ube2t	ubiquitin-conjugating enzyme E2T	E2 ubiquitin/ISG15 conjugating enzyme	2.3↑
Ube2L6	ubiquitin-conjugating enzyme E2L6	E2 ubiquitin/ISG15 conjugating enzyme	2.3↑
Protein kinase R pathway			
Eif2a	eukaryotic translation initiation factor 2α	subunit of guanylate exchange factor	NSA
Eif2ak(PKR)	protein kinase R	eIF2α kinase	NSA

Appendix 2 continued

2-5 oligoadenylate synthetase/RNase L pathway			
Oasl2	2',5'-oligoadenylate synthetase-like 2	cytosolic viral RNA receptor/oligoadenylate synthetase	75.9↑
Oasl	2',5'-oligoadenylate synthetase-like	cytosolic viral RNA receptor/oligoadenylate synthetase	43.5↑
Oas1b	2',5'-oligoadenylate synthetase 1b	cytosolic viral RNA receptor/oligoadenylate synthetase	36.9↑
Oas1i	2',5'-oligoadenylate synthetase 1	cytosolic viral RNA receptor/oligoadenylate synthetase	13.6↑
Oas1a	2',5'-oligoadenylate synthetase 1a	cytosolic viral RNA receptor/oligoadenylate synthetase	11.7↑
Oas2	2',5'-oligoadenylate synthetase 2	cytosolic viral RNA receptor/oligoadenylate synthetase	5.7↑
Rnase L	ribonuclease L	ssRNA endonuclease	5.7↑
Guanylate-binding proteins			
Gbp5	guanylate-binding protein 5	GTPase	75.8↑
Gbp1	guanylate-binding protein 1	GTPase	61.2↑
Mx1	myxovirus resistance protein 1	GTPase	51.0↑
Irgm	immunity-related GTPase M	GTPase	45.5↑
10801975	similar to IFN-inducible GTPase	GTPase (putative)	33.7↑
10819545	similar to guanylate binding protein 1, IFN-inducible, 67kDa	GTPase (putative)	33.3↑
Gbp4	guanylate-binding protein 4	GTPase	32.1↑
Gbp2	guanylate-binding protein 2	GTPase	21.1↑
Mx2	myxovirus resistance protein 2	GTPase	15.7↑
10801973	similar to IFN-inducible GTPase	GTPase (putative)	15.6↑
Irg1 (p47GBP)	p47 guanylate-binding protein	GTPase	14.8↑

Appendix 2 continued

Other type I IFN-regulated genes			
Rsad2	radical S-adenosyl methionine domain containing 2	viperin/antiviral protein	100.0↑
Cxcl11	C-X-C motif ligand 11	chemokine	98.7↑
Ifit1	IFN-induced protein with tetratricopeptide repeats 1	translation regulator	91.4↑
Ifit2	IFN-induced protein with tetratricopeptide repeats 2	translation regulator	85.8↑
Ifit3	IFN-induced protein with tetratricopeptide repeats 3	translation regulator	41.0↑
Cd274 (PD-L1)	cluster of differentiation 274 (programmed cell death ligand 1)	cytokine/suppressor of immune system	34.4↑
10720237	similar to IFN λ2	cytokine/type III IFN (putative)	23.0↑
Il15	interleukin 15	cytokine	17.3↑
Isg20	exonuclease	exonuclease	7.0↑
Adar	adenosine deaminase, RNA specific	RNA editing enzyme/antiviral protein	4.9↑
Adarb1	adenosine deaminase, RNA specific b1	RNA editing enzyme/antiviral protein	2.0↓
Type II IFN effector pathways			
Ifi47	IFNγ inducible protein 47	Ras-like GTPase	78.1↑
Gbp5	guanylate-binding protein 5	GTPase	75.8↑
Gbp1	guanylate-binding protein 1	GTPase	61.2↑
Cxcl9	C-X-C motif ligand 9	chemokine	48.9↑
Irgm	immunity-related GTPase M	Ras-like GTPase	45.5↑
Oasl	2'-5'-oligoadenylate synthetase-like	cytosolic viral RNA receptor/OAS	43.5↑
Gbp4	guanylate-binding protein 4	GTPase	32.1↑
Gbp2	guanylate-binding protein 2	GTPase	21.1↑
Cxcl10	C-X-C motif ligand 10	chemokine	18.1↑
Irf1	IFN regulatory factor 1	transcription factor	17.5↑
Tnfsf10 (TRAIL)	TNF superfamily 10	inflammatory cytokine	17.3↑
Il15	interleukin 15	cytokine	17.3↑
Ccl4	C-C motif ligand 4	chemokine	16.8
Igtp	IFNγ-induced GTPase	GTPase	11.8↑
Nos2	inducible nitric oxide synthase	nitric oxide synthase	6.9↑
Irf9	IFN regulatory factor 9	transcription factor	6.2↑
Adar	adenosine deaminase, RNA specific	RNA editing enzyme	4.9↑
Irf8	IFN regulatory factor 8	transcription factor	3.9↑

For footnotes see Appendix 1.

Appendix 3 Expression of genes stimulating cell proliferation

Gene	Protein	Protein function	Induction/ repression by MTH-68/H (fold) [a,b]
Efna1	ephrin A1	growth factor	2.0↓
Ccne1	cyclin E1	regulator of G1/S transition	2.1↓
EphB2	ephrin receptor B2	receptor tyrosine protein kinase	2.1↓
Bmp7	bone morphogenic protein 7	TGF-β family	2.1↓
Uhrf1	ubiquitin-like with PHD and ring finger domains 1	regulator of G1/S transition	2.2↓
Tubb3	tubulin, beta 3	mitotic spindle component	2.2↓
Cdc20	cell division cycle 20	component of anaphase promoting complex	2.3↓
Cdc45l	cell division cycle 45-like	regulator of initiation of replication	2.3↓
Cenpa	centromere protein A	centromeric histone H3 variant	2.3↓
Cdc25B	cell division cycle 25 B	protein tyrosine phosphatase	2.4↓
Mina	myc-induced nuclear antigen	regulator of cell growth	2.5↓
Cdc26	cell division cycle 26	component of anaphase promoting	2.6↓
Pola2	polymerase (DNA-directed), α2	complex	2.6↓
Haus1	HAUS augmin-like complex, subunit 1	DNA polymerase subunit	2.6↓
Dixdc1	dishevelled-axin domain containing 1	mitotic spindle assembly	2.6↓
Ccnjl	cyclin J-like	regulator of cell cycle	2.6↓
Bmyc	Myc family protein	regulator of cell cycle	2.6↓

Appendix 3 continued

Gene	Protein	Protein function	Induction/ repression by MTH-68/H (fold) a ,b,
Dctd	deoxycytidylate deaminase	regulator of cell cycle	2.7↓
Mif4gd	MIF46 domain containing	enzyme of nucleotide metabolism	2.7↓
Sept3	septin 3	regulator of histone synthesis	2.8↓
Fgf11	fibroblast growth factor 11	growth factor	2.9↓
Figf (VEGFD)	c-fos induced growth factor (vascular endothelial growth factor D)	angiogenic growth factor	3.0↓
Pole2	polymerase (DNA-directed), ε2	DNA polymerase subunit	3.1↓
Nme7	non-metastatic cells 7	nucleoside diphosphate kinase	3.5↓
Rpa3	replication protein A3	DNA polymerase subunit	3.2↓

For footnotes see Appendix 1.

Appendix 4 Expression of genes inhibiting cell proliferation

Gene	Protein	Protein function	Induction/ repression by MTH-68/H (fold) a ,b,
10860801	similar to OEF2/Samd9	inhibitor of cell growth (putative)	64.7↑
Slfn3	schlafen 3	inhibitor of tumor invasion	38.6↑
Cnksr3	connector enhancer of kinase suppressor of ras 3	scaffold protein/inhibitor of Ras/ERK pathway	15.2↑
Samd9l	sterile alpha motif domain containing 9-like	inhibitor of cell growth	11.1↑
Slfn5	schlafen 5	regulator of cell growth	10.9↑
Ido1	indoleamine 2,3-dioxygenase 1	enzyme of tryptophan metabolism	6.0↑
Btg2	B-cell translocation gene 2	inhibitor of cell cycle	3.2↑
Klf10	Krüppel-like factor 10	inhibitor of cell cycle	2.2↑
Dusp1	dual specificity phosphatase 1	MAPK phosphatase	2.1↑
E2f6	E2F transcription factor 6	inhibitor of G1/S transition	2.1↓
Mdc1	mediator of DNA damage checkpoint 1	mediator of S-, G2/M arrest	2.1↓
Cdkn2c	cyclin-dependent kinase inhibitor 2C (p18)	Cdk4/6 inhibitor	2.2↓
Rbl2	retinoblastoma-like 2	regulator of histone H4 methylation and cell cycle	2.3↓

For footnotes see Appendix 1.

Appendix 5 Expression of genes of intrinsic apoptosis in MTH-68/H-infected PC12 cells

Gene	Protein	Protein function	Induction/ repression by MTH-68/H (fold) [a,b]
Apaf1	apoptotic peptidase activating factor 1	scaffold protein component of apoptosome	4.6↑
Bid	BH3 interacting domain death agonist	pro-apoptotic Bcl2 family protein	2.6↑
Casp7	caspase-7	effector caspase	2.6↑
Cyc1	cytochrome c-1	apoptosis regulator	NSA[c]
Casp9	caspase-9	initiator caspase	NSA
Casp3	caspase-3	effector caspase	NSA
Bad	Bcl-2-associated death promoter	pro-apoptotic Bcl2 family protein	NSA
Bim	Bcl-2 interacting mediator of cell death	pro-apoptotic Bcl2 family protein	NSA
Bcl-2	B cell lymphoma-2	anti-apoptotic Bcl2 family protein	NSA
Bcl-xl	B cell lymphoma-extra large	anti-apoptotic Bcl2 family protein	NSA
Mcl-1	myeloid cell leukemia sequence-1	anti-apoptotic Bcl2 family protein	NSA
Bak	Bcl-2 homologous antagonist killer	pro-apoptotic Bcl2 family protein	NSA
Bax	Bcl-2 associated protein	pro-apoptotic Bcl2 family protein	NSA
Tp53	tumor protein 53	transcription factor/tumor suppressor	NSA
Noxa/Pmaip1	PMA-induced protein 1	pro-apoptotic Bcl2 family protein	NSA
Puma	p53-upregulated modulator of apoptosis	pro-apoptotic Bcl2 family protein	ND

For footnotes see Appendix 1.

Appendix 6 Expression of genes of extrinsic apoptosis in MTH-68/H-infected PC12 cells

Gene	Protein	Protein function	Induction/ repression by MTH-68/H (fold) [a,b]
Tnf	tumor necrosis factor (TNF superfamily, member 2)	cytokine	35.4↑
Tnfsf10 (TRAIL)	TNF superfamily, member 10 (TNF-related apoptosis inducing ligand)	cytokine	17.3↑
Ripk2	receptor-interacting serine-threonine kinase 2	serine-threonine kinase	8.4↑
Birc3 (cIAP2)	baculovirus IAP repeat-containing 3 (cellular inhibitor of apoptosis protein 2)	adapter protein	6.1↑
Lta	lymphotoxin alpha (TNF superfamily, member 1)	cytokine	6.0↑
Birc2 (cIAP1)	baculovirus IAP repeat-containing 2 (cellular inhibitor of apoptosis protein 1	adapter protein	3.5↑
Tnfsf15	tumor necrosis factor superfamily, member 15	cytokine	3.0↑
Traf2	Tnf receptor-associated factor 2	E3 ubiquitin ligase/adapter protein	2.6↑
Ripk3	receptor-interacting serine-threonine kinase 3	serine-threonine kinase	2.5↑
Fas	Fas (TNF receptor superfamily, member 6)	cytokine receptor	2.3↑
Faslg	Fas ligand (TNF superfamily, member 6)	cytokine	2.2↑
Ripk1	receptor-interacting serine-threonine kinase 1	serine-threonine kinase	NSA
Tnf-r1	TNF receptor 1	cytokine receptor	NSA
Casp8	caspase-8		NSA
Fadd	Fas-associated death domain protein	initiator caspase	NSA
Tradd	TNF receptor-associated death domain protein	adapter protein	2.0↓
Trail-r1	TRAIL receptor 1	adapter protein	2.2↓
Trail-r2	TRAIL receptor 2	cytokine receptor	ND
		cytokine receptor	ND

For footnotes see Appendix 1.

Appendix 7 Expression of genes of ER stress pathway in MTH-68/H-infected PC12 cells

Gene	Protein	Protein function	Induction/ repression by MTH-68/H (fold) [a,b]
Atf3	activating transcription factor 3	transcription factor	40.1↑
Casp4	caspase-4	initiator caspase	14.0↑
Casp12	caspase-12	initiator caspase	11.8↑
Ddit3(CHOP)	DNA damage inducible transcript 3 (C/EBP homology protein)	transcription factor	3.4↑
Traf2	TNF receptor-associated factor 2	adapter protein	2.6↑
Bip	binding Ig heavy chain protein	ER chaperone	NSA
Perk	PKR-like endoplasmic reticulum kinase	UPR sensor/serine-threonine kinase	NSA
Ire1	inositol-requiring enzyme 1	UPR sensor/endoribonuclease	NSA
Atf6	activating transcription factor 6	UPR sensor/transcription factor	NSA
Xbp1	X-box binding protein 1	transcription factor	NSA
Nrf2	nuclear factor (erythroid-derived 2)-related factor 2	transcription factor	NSA
Jnk	c-Jun N-terminal kinase	serine-threonine kinase	NSA
Atf4	activating transcription factor 4	transcription factor	NSA
Ask1	apoptosis stimulating kinase 1	serine-threonine kinase	ND

For footnotes see Appendix 1.

11 Acknowledgement

I would like to acknowledge all of the help provided by my tutor, Dr. Marianna Pap who invited me to the fascinating world of CREB, guided and supported me during my Ph.D. studies. I would also like to express my acknowledgement to Professor Szeberényi as he provided a notable support and gave me advice whenever it was required.

Furthermore I would like to thank the great work, help and fun for the other colleagues of the MACIM work group, namely Mária Németh and Ibolya Koloszár, without them this thesis would not exist.

Additionally I would like to thank the contribution of all of the members of the Department of Medical Biology, Faculty of Medicine, University of Pécs.

I am extremely thankful for Dr. Zoltán Rékási and Dr. Beáta Polgár for the quick and precise pre-check of the thesis helping to succeed to the final version of these pages.

I would like to express my gratitude to Prof. Müller for his support and making possible to perform a significant part of the experiments in his laboratory.

And last but not least I would like to thank the help and support my family and all of the friends.

12 Publication list

The thesis is based on the following publications:

Balogh, A., J. Bator, L. Marko, M. Nemeth, M. Pap, G. Setalo, Jr., D. N. Muller, L. K. Csatary, and J. Szeberenyi. "Gene Expression Profiling in Pc12 Cells Infected with an Oncolytic Newcastle Disease Virus Strain." *Virus Res* 185, (2014): 10-22.

IF 2012: 2.745

Balogh, A., M. Nemeth, I. Koloszar, L. Marko, L. Przybyl, K. Jinno, C. Szigeti, M. Heffer, M. Gebhardt, J. Szeberenyi, D. N. Muller, G. Setalo, Jr., and M. Pap. "Overexpression of Creb Protein Protects from Tunicamycin-Induced Apoptosis in Various Rat Cell Types." *Apoptosis* 19, no. 7 (2014): 1080-98.

IF 2012: 3.949

The thesis is based on the following conference presentations abstracts and essays:

Balogh, A. M. Pap, A simple fluorescent labeling technique to study virus adsorption in Newcastle disease virus infected cells - A novel method to label and track enveloped virus particles, Tecan Young Researcher Award, Budapest, 2011, *oral presentation*

Balogh, A. M. Pap, A CREB transzkripciós faktor szerepe PC12 sejtek neuronális differenciációjában és túlélésében, Conference of Biologist Doctorandi, Pécs, 2009, *oral presentation*

Balogh., A., M. Pap., J. Szeberenyi, CREB foszforilációs helyek szerepe PC12 sejtek proliferációjában, PhD Scientific Days, Budapest, 2009, *oral presentation*

Stark, B., A. Harci, **A. Balogh,** G. Berta, G. Setalo Jr., J. Szeberényi, Egy peptidil-aldehid proteaszóma gátló (MG-131) jelátviteli hatásainak vizsgálata patkány feokromocitóma (PC12) sejtekben, PhD Scientific Days, Budapest, 2007, *poster*

Balogh, A., Z. Németh, B. Stark, A. Harci, A CREB fehérje 129-es és 133-as szerin aminosavainak szerepe PC12 sejtek proliferációjában, XII. Frigyes Korányi Scientific Forum, Budapest, 2007, *oral presentation*

Balogh, A., Proliferative effect of the CREB protein in PC12 cells, YES Young European Scientist 2nd Meeting, Porto, 2007, *poster*

Balogh, **A.**, Z. Nemeth, A. Harci, B. Stark, Proliferative effect of Ser-129 and Ser-133 phosophorilation sites in the CREB protein, ISCOMS - 14th Internation Student Congress of Medical Sciences, Groeningen, 2007, *poster*

Balogh, A., Z. Németh, A. Harci, B. Stark, Proliferative role of Ser-129 and Ser-133 in the CREB protein, CROSS - 3rd Croatian Student Summit, Zagreb, 2007, *oral presentation*

Balogh, A., B. Stark, A. Harci, Z. Németh, A CREB transzkripciós faktor Ser-129-es és Ser-133-as foszforilációs helyeinek szerepe PC12 sejtek proliferációjában, V. Interdisciplinary Grastyán Conference, Pécs, 2007, *oral presentation*

Balogh, A., A CREB transzkripciós faktor Ser-129 és Ser-133 aminosavak foszforilációjának szerepe PC12 sejtek differenciációjában és túlélésében, XI. Frigyes Korányi Scientific Forum, Budapest, 2006, *oral presentation*

Balogh, A., M. Pap, Z. Nemeth, B. Stark, A. Harci, J. Szeberenyi, A CREB transzkripciós faktor Ser129 és Ser133 aminosavak foszforilációjának szerepe PC12 sejtek neuronális differenciációjában, proliferációjában és túlélésében, XIV. Cell and Development Biology Days, Balatonfüred, 2006, *poster*

Balogh, A., A CREB transzkripciós faktor szerepe PC12 sejtek proliferációjában, PTE ÁOK TDK Conference, Pécs, 2006, *oral presentation*

Pap, M., **A. Balogh**, A CREB transzkripciós faktor szerepe PC12 sejtek differenciációjában és apoptózisában, XIII. Cell and Development Biology Days, Eger 2005, *oral presentation*

Balogh, **A.**, A CREB transzkripciós faktor szerepe PC12 sejtek neuronális differenciációjában és apoptózisában, XXVII. OTDK, Szeged, 2005, *oral presentation*

Balogh, A., A CREB transzkripciós faktor szerepe PC12 sejtek neuronális differenciációjában és apoptózisában, PTE ÁOK TDK Conference, Pécs, 2005, *oral presentation*

Balogh, A., A CREB transzkripciós faktor szerepe PC12 sejtek differenciációjában és túlélésében, PTE ÁOK Dean's Essay, Pécs, 2004, *essay*

Balogh, A., A CREB transzkripciós faktor szerepe PC12 sejtek differenciációjában és túlélésében, PTE ÁOK TDK Conference, Pécs, 2004, *oral presentation*

Conference abstracts, presentations and posters not related to the thesis:

Magyar, K., A. Riba, Z. Vamos, **A. Balogh**, L. Deres, T. Kalai, K. Hideg, L. Seress, B. Sümegi, A. Koller, R. Halmosi, K. Toth, Az Akt és a MAP-kináz rendszer szerepe krónikus hipertenzív patkány modellben a PARP gátlás által kiváltott védelemben, FAME, Pécs, 2011, *poster*

Magyar, K., A. Riba, Z. Vamos, **A. Balogh**, L. Deres, T. Kalai, K. Hideg, L. Seress, B. Sümegi, A. Koller, R. Halmosi, K. Toth, The role of Akt and mitogen-activated protein kinase systems int he protective effect of PARP inhibition in a chronic hypertensive rat model, Cardiologia Hungarica 2011, 41: (Suppl F) p.F37

Magyar, K., Z. Vamos, K. Bruszt, **A. Balogh**, T. Kalai, K. Hideg, L. Seress, B. Sumegi, A. Koller, R. Halmosi, K. Toth, Inhibition of Poly(ADP-ribose) polymeras ereduces hypertension induced vascular remodeling in spontaneous hypertensive rat model. Second international Symposium on Hypertension, november 18-21, 2010, Osijek, Croatia, Kidney and Blood Pressure Research 2010; 33: 425

Magyar, K., A Riba, Z. Vamos, **A. Balogh**, L. Deres, K. Hideg, B. Sumegi, A. Koller, R. Halmosi, K. Toth, The role of Akt and mitogen-activated protein kinase systems in the vasoprotection elicited by PARP inhibition in hypertensive rats, European Socitey of Congress, Paris, France, 27, Eur. Heart J, 32 (Abstract Supplement), 34, 2011.

Magyar, K., A Riba,, K. Bruszt, **A. Balogh**, K. Hideg, L. Seress, B. Sumegi, K. Toth, R. Halmosi, Az L-2286 jelű PARP-gátló vegyület lehetséges szerepe a miokardialis őssejt regenerációban. Magyar Kardiológusok Társasága 2012. évi Tudományos Kongresszusa, 2012. május 9-12. Card. Hung. Suppl. A., 42:A30.

Deres, L., K. Magyar, I. Takacs, K. Eros, **A. Balogh**, K. Hideg, B. Sumegi, K. Toth, R. Halmosi, A PARP-gátlás csökkenti a vaszkuláris fibrózist spontán hipertenzív patkánymodellben Magyar Kardiológusok Társasága 2012. évi Tudományos Kongresszusa, 2012. május 9-12. Card. Hung. Suppl. A., 42: A21

Magyar, K., I. Takacs, K. Bruszt, **A. Balogh**, K. Hideg, L. Seress, B. Sumegi, R. Halmosi, K. Toth The potencial role of a PARP-inhibitor in the myocardial stem cell regeneration, Congress of European Society of Cardiology, Munich, Germany, 25 Aug 2012 - 29 Aug 2012, Eur. Heart J, 2012, 33 (Suppl. 1)

Journal publications not related to the thesis:

Balogh, A., M. Pap, L. Marko, I. Koloszar, L. K. Csatary, and J. Szeberenyi. "A Simple Fluorescent Labeling Technique to Study Virus Adsorption in Newcastle Disease Virus Infected Cells." *Enzyme Microb Technol* 49, no. 3 (2011): 255-9.

IF: 2.367

Berta, G., A. Harci, O. Tarjanyi, M. Vecsernyes, **A. Balogh**, M. Pap, J. Szeberenyi, and G. Setalo, Jr. "Partial Rescue of Geldanamycin-Induced Trka Depletion by a Proteasome Inhibitor in Pc12 Cells." *Brain Res* 1520, (2013): 70-9.

IF 2012: 2.879

Magyar, K., L. Deres, K. Eros, K. Bruszt, L. Seress, J. Hamar, K. Hideg, **A. Balogh**, F. Gallyas, Jr., B. Sumegi, K. Toth, and R. Halmosi. "A Quinazoline-Derivative Compound with Parp Inhibitory Effect Suppresses Hypertension-Induced Vascular Alterations in Spontaneously Hypertensive Rats." *Biochim Biophys Acta* 1842, no. 7 (2014): 935-944.

IF 2012: 4.910

Mikolas, E., J. Cseh, M. Pap, I. A. Szijarto, **A. Balogh**, B. Laczy, V. Beko, V. Fisi, G. A. Molnar, A. Merei, J. Szeberenyi, and I. Wittmann. "Effects of Erythropoietin on Glucose Metabolism." *Horm Metab Res* 44, no. 4 (2012): 279-85.

IF: 2.145